

Chapter 4

Plant mediated synthesis of Copper oxide and Silver nanoparticles: Application in catalysis and biological studies

4.1 Introduction

Nanotechnology and natural science mutually depend on each other. Nanotechnology provides tool for the development of biological systems whereas natural science provides bio assembled components to nanotechnology. The synthesis of nanoparticles were carried out by different methods; physical, chemical and biological. Biosynthetic methods offers greener, eco-friendly and economical procedures for the synthesis of nanoparticles using microorganisms and enzymes. Plant or plant parts are also used for the fabrication of nanoparticles as they contain antioxidant as secondary metabolites.

Silver nanoparticles are known to possess unique electrical, optical and biological properties. In addition they find application in catalysis, drug delivery, sensing field etc. As a consequence of possessing antimicrobial¹ and antibacterial² activity silver gains more attention than other metals. Copper based compounds can promote various reactions while they can exhibit different oxidation state such as Cu^0 , Cu^I , Cu^{II} , Cu^{III} . They find application in various field like nanotechnology, electrocatalysis and catalyst in organic transformations.³⁻⁵ Now a days, biosynthesis of nanoparticle have gained much attention due to

- i) Use of aqueous solvent
- ii) Simple procedure
- iii) Phytoconstituents act as both reducing and stabilizing agent
- iv) Eco-friendly
- v) Easy availability

4.2 Synthesis and Application of nanoparticles- A Review

Recently, nanotechnology is an emerging field in chemistry which come up with wide variety of applications because of the geometry, shape and morphology of nanoscale materials.⁶ Nanoscale material may be nanorods, nanotubes, nanoparticle and nanowires etc. The specific features of nanoparticles such as small size, high surface-volume ratio etc gave them more priority than the bulk materials in many applications. Metallic nanoparticle found out its application in various fields like cosmetics, electronics, biotechnology, coatings, therapeutic, biomedical field etc. Traditional procedure for the synthesis of nanoparticle involves wet chemical method, microemulsion, photocatalytic etc. Wet chemical method is recently upgraded as sol-gel method which produces uniform nanostructured materials with high purity even at low temperature. However the use of toxic solvents and the generated by-products in this method are hazardous to environment and health. Therefore, synthesis of nanoparticles by this method is much less in the developing world.^{7,8} In order to avoid the drawbacks and to make the reaction green, the biosynthesis of nanoparticle came into existence. Here bio stands for the varieties of available biological sources in nature like plants, plant parts, yeast, fungi, algae, bacteria and virus. A brief discussion on different methods commonly used for the synthesis of nanoparticle is given below.

Chemical reduction

For the bulk synthesis of nanoparticle, chemical reduction of metal salt can be used.⁹ This method is also known as wet method as it occurs in liquid medium. The reaction requires the presence of three major components

- i) Metal precursor
- ii) Reducing agent and
- iii) Stabilizing agent

The reduction of metal precursor using suitable reducing agent and in presence of a stabilizing agent can prevent the aggregation of synthesized nanoparticles. According to LaMer-Dinegar model¹⁰ during the period of nucleation a number of colloidal particles will be formed and remain unchanged. Further growth of the particles will take place by the reduction of metal ion on the surface of clusters formed during the

nucleation period. Nucleation and growth of nuclei can be controlled by adjusting the reaction parameters like pH, temperature, metal precursor, reducing as well as stabilizing agent. By controlling the nucleation and growth, one can synthesize monodispersed nanoparticles i.e. the nanoparticles with uniform size distribution. Since nanoparticles possess large surface area, they have the tendency to form clusters and large particles. To prevent aggregation usually organic compounds like surfactants, organic polymer, dendrimers, stabilizing agents etc are used.¹¹⁻¹⁵ Chemical reduction method again is subdivided into six types according to the reducing agent used for the nanoparticle synthesis; i) citrate reduction method,¹⁶⁻²³ ii) reduction using NaBH_4 ,²⁴⁻²⁶ iii) polyol reduction method,²⁷⁻²⁹ iv) reduction using ascorbic acid,³⁰⁻³⁵ v) reduction using DMF^{36,37} and vi) hydroxyl amine reducing agent.³⁸ Like every other procedures, chemical reduction method also had some advantages and disadvantages. The major advantages are faster reaction rate, no need of special experimental setup, large scale synthesis. By controlling the reaction conditions like temperature, pressure, pH etc one can synthesize nanoparticles in desired size, shape whereas the use of toxic chemicals produce both environmental and health hazards.

Microemulsion Method

A microemulsion consists of ternary systems such as water, oil which is an immiscible liquids and surfactant or quaternary mixture which contains an additional reagent which acts as co-surfactant. Here the surfactant molecules form a monolayer at the interface between water and oil where hydrophobic tail dissolved in oil and hydrophilic heads in aqueous phase. In this method, both nucleation and growth of nanoparticles take place within the aqueous phase. By adjusting the water-to-surfactant ratio the droplet dimensions can be maintained. Agglomeration of nanoparticle can be controlled by the surfactant molecule by adsorbing on to the nanoparticle surface. Surfactants are classified into anionic, cationic and nonionic depending on the charges of polar head group. Anionic surfactant produces nanoparticles with smaller and narrow size distribution. Commonly used anionic surfactant are bis(2-ethylhexyl) sulfosuccinate (AOT), sodium dodecyl benzene sulfonate (SDBS) and sodium lauryl sulfate (SLS). CTAB (cetyltrimethylammonium bromide) is used as cationic surfactant whereas Triton X-100 is used as nonionic

surfactant. Major advantages of this method is the uniform size and morphology of the synthesized nanoparticle.³⁹ Drawback include the difficulty in the removal and separation of solvent from the nanoparticle

Sonochemical method

Introducing ultrasound in nanoparticle synthesis has the effect of producing very small and stable nanoparticles. The ultrasound energy can cause the rupture of chemical bonds thereby forming radicals which act as reducing agent. For examples, when the synthesis was carried out in aqueous medium, water molecules split into hydrogen and hydroxyl radicals which act as reducing agent for metal ion.⁴⁰ Gadanken reported the synthesis of copper nanoparticle using both thermal and sonochemical method⁴¹ in which copper(II) hydrazine carboxylate was used as precursor. Thermal reduction yields pure metallic copper as product whereas both copper and copper(I) oxide are produced in sonochemical reduction. This may be attributed by the *in situ* oxidation of copper by H₂O₂ which is generated under sonochemical conditions. Thermally derived nanoparticles shows the presence of irregularly shaped copper nanoparticle whereas sonochemical method produces a porous aggregate of irregular shaped nanoparticles. Gadanken again reported the synthesis of amorphous copper and nanocrystalline copper oxide embedded in polyaniline matrix using sonochemical reduction method.⁴² Salkar reported the synthesis of silver nanoparticle by sonochemical reduction of silver nitrate for 1h sonication.⁴³

Photochemical method

This method produces metal nanoparticle either by the direct photoreduction of metal precursor or by the reduction of photochemically generated intermediates like radicals. The photochemical synthesis of copper nanoparticle incorporated in poly(vinyl pyrrolidone) which act as protecting agent and bis(2,4-pentandionato)copper(II) complex used as metal precursor.⁴⁴ Advantages of such synthesis are clean synthesis, controllable generation of reducing agents, versatility etc.

The above methods have the drawbacks like use of toxic chemicals, nonpolar organic solvents and the use of stabilizing and capping agents. To avoid these problems,

researchers developed green synthesis of nanoparticles using biomaterials which are eco-friendly and provide clean procedure .

Biosynthesis of nanoparticle

For the eco-friendly synthesis of nanoparticles biological method was developed. The major sources for the synthesis of nanoparticle are bacteria, fungi and plant extracts. The biosynthesis is generally a bottom up approach involving the reduction and oxidation reactions.

Synthesis of nanoparticle from bacteria

For the first time, synthesis of silver nanoparticle was reported from *Pseudomonas stutzeri*.⁴⁵ The bacteria were grown in Lennox L broth containing 50 mM AgNO₃ at 30 °C for 48 h in dark. The formation of silver nanoparticle was confirmed by TEM and EDX analysis. Reduction of silver ions by *Klebsiella pneumonia*, *E. coli*, and *Enterobacter cloacae* (*Enterobacteriaceae*) were reported.⁴⁶

Polydispersed silver nanoparticles were synthesized from *Geobacillus stearothermophilus* by Fayaz.⁴⁷ High stability of this nanoparticle is attributed to the secretion of capping agent produced by the bacterium. Kalishwarala reported the synthesis of nanoparticle using *Brevibacterium casei* from dairy waste.⁴⁸ Wet *B. casei* along with silver nitrate incubated in an incubator was stirred at 37 °C for 24 h. The SPR of silver nanoparticle was observed at 420 nm with average particle size of 10-50 nm. *Bacillus* strain CS-11 obtained from industrial area was used for the production of silver nanoparticles.⁴⁹ The formation of nanoparticle at room temperature within 24 h was confirmed by UV-vis absorption at 450 nm. TEM analysis suggested that the nanoparticle is having an average size between 42-92 nm.

Synthesis of nanoparticle from fungus

Due to the secretion of large amounts of enzymes by fungi than bacteria, fungus can be used for the synthesis of nanoparticles. Possible steps for the synthesis of nanoparticle includes: trapping of silver ions at the surface of fungal cells followed by the subsequent reduction of silver ions by the enzymes present in fungus. Extracellular enzymes naphthaquiniones and anthraquinones are responsible for such reduction process. Synthesis of silver nanoparticle was reported using fungus

*Verticillium*⁵⁰ by the intracellular reduction of silver ions to silver nanoparticle with an average dimension of 25±12 nm. Ahmad *et.al* reported the extracellular synthesis of silver nanoparticle using fungus *Fusarium oxysporum*. The synthesized nanoparticle were stabilized by the proteins secreted by fungus.⁵¹ Using nitrate reductase enzyme from *Fusarium oxysporum* silver nanoparticle was synthesized in presence of a co-factor NADPH.⁵² The synthesis involves the incubation of silver nitrate, phytochelatin, 4-hydroxyquinoline and NADPH at 25 °C for 5 h under anaerobic conditions. *Penicillium fellutanum* mediated synthesis of silver nanoparticle was reported by Kathiresan where the silver ions mixed with cell filtrate and agitated at 25 °C under dark conditions.⁵³

Biosynthesis of nanoparticle using Plant

Bio fabrication of nanoparticle using plant can be easily understood by dividing it into two categories i) intracellular synthesis and ii) extracellular synthesis. In intracellular synthesis aqueous solution of metal salt was treated with living plant or plant biomass producing metal nanoparticle and the recovery of nanoparticle was done by cell rupture. Extracellular synthesis involves the treatment of aqueous solution of metal salt with aqueous plant extract and the nanoparticles can be collected by centrifugation from the resultant colloidal solution. Treatment of individual phytoconstituent with aqueous metal salt solution results in metal ion reduction and purification of nanoparticle was done by ion exchange chromatography. There are few reports available which shows the isolation of particular phytoconstituents and used for the synthesis of nanoparticles.⁵⁴⁻⁵⁹

Living Plant Mediated Synthesis (Intracellular synthesis)

The living plant contains heavy metal accumulation and this strategy can be used for synthesis. Yacaman reported the synthesis of silver nanoparticle from *Alfalfa sprouts*⁶⁰ using silver nitrate as precursor. In 2008 Harris studied the extent of metal ion formation and uptake in *Brassica juncea* and *M. sativa*.⁶¹ Similarly gold nanoparticles were synthesized from plant biomass.^{62,63} Main disadvantage of the procedure is the tedious recovery step of nanoparticle and the availability of reducing and stabilizing bioorganic compounds which varies according to different parts. The size and morphology variation of nanoparticle being observed in such cases is

attributed to the difficulties associated with the separation and purification procedures.

Plant Extract Mediated synthesis of nanoparticle (Extracellular synthesis)

Plant contains variety of phytoconstituents which are responsible for the reduction of metal ions. In extracellular process these phytoconstituents are extracted and exploited directly for the synthesis of metallic nanoparticles. It is very rare to produce nanoparticles with monodispersity and definite morphology as a result of variation of the phytoconstituents in plants and presence of impurities. Plant extract mediated synthesis supports the formation of spherically shaped and highly reactive nanoparticle. By controlling the reaction conditions in plant extract mediated synthesis one can produce nanoparticle for commercial application. It has been reported by many academics that high polydispersity index of such synthesis is due to the variation of phytoconstituents.

Ibrahim reported the synthesis of silver nanoparticle from banana peel extract in 2015.⁶⁴ Banana peel extract [BPE] act as reducing as well as capping agent. He studied different factors like optimum concentration, pH and incubation time. Metal salt concentration as well as BPE concentration influences the synthesis of nanoparticle which could be understood from the observation of color change from light reddish brown color to dark reddish brown color. The reddish brown color is attributed to the Surface Plasmon Resonance (SPR) with characteristic SPR band at λ 433 nm. Other conditions such as at pH 2, reduction of silver ions doesn't take place which is confirmed by the absence of SPR band. Similarly at low temperature reduction occurs slowly that the development of reddish brown color appears only after 10min. Synthesized silver nanoparticle revealed good antimicrobial activity.

Lee *et.al* developed an efficient method for the synthesis of silver nanoparticle from *Myrsitica fragrans* seed extract, and found to have an excellent antimicrobial activity.⁶⁵ The characteristic surface plasmon resonance was observed at 410 nm corresponds to the reduction of silver ions to silver nanoparticles. The size of the Ag nanoparticle was found out using TEM and it was in the range of 7-20 nm size. The XRD patterns suggest the formation of metallic silver which has FCC structure. Antimicrobial activity of silver nanoparticles against both gram negative and gram-

positive bacteria was found to be concentration dependent, as the concentration of nanoparticle increases microbial growth decreases.

Biogenic synthesis and characterization of silver nanoparticle using *Memecylon edule* leaf extract were done by Elavazhagan and Arunachalam under dark condition.⁶⁶ They observed UV absorption peak at 475 nm. SEM results showed the silver nanoparticles have an average diameter of 50-90 nm. At room temperature synthesis of silver nanoparticle was carried out using *Argemone Mexicana*⁶⁷ within 4 h. They observed characteristic UV absorption peak at 440 nm. The XRD pattern shows that the silver nanoparticle contains both cubic and hexagonal structures. The silver nanoparticles produced were found to be toxic against the bacteria *Escherichia coli*, *Pseudomonas syringae* and the fungi *Aspergillus flavus*.

Carica papaya fruit extract was used for silver nanoparticle synthesis by Kothari.⁶⁸ Room temperature reduction of silver ions was carried out by Papaya fruit extract within 5 h and they got SPR band at 450 nm with broadening indicating the polydispersity of silver nanoparticles. Formation of silver nanoparticles was further confirmed by XRD measurements which produces characteristic peaks of metallic silver having both cubic and hexagonal structures. IR spectrum of both plant extract and silver nanoparticles confirms the role of polyols in the reduction of silver ions. Characteristic -C-O group peak of polyols was found to be absent after the bioreduction and they concluded that such polyols will be responsible for the reduction of silver ions. At a concentration of 50 ppm, silver nanoparticles exhibit anti bacterial activity against *E. coli* and *Pseudomonas aeruginosa*.

Yugandhar P. reported the synthesis of silver nanoparticle from fruit extract of *Syzygium alternifolium*.⁶⁹ Here formation of silver nanoparticles was confirmed by observing the color change from brown to grey. The SPR band of UV-Visible spectrum at 442 nm again confirms the formation of silver nanoparticles. This band corresponds to primary amines and proteins that are interacted with silver NPs and act as reducing agent. Surface topology of nanoparticle was studied by AFM analysis, which shows a spherical shape for silver NPs and the size is in the range of 32-68 nm as confirmed by SEM analysis. TEM analysis identifies the polydispersity nature of the silver nanoparticles without any agglomeration.

Ocimum sanctum (Lakshmi tulasi) which had medicinal values being a principal herb of ayurveda and used as reducing agent for the bioreduction of silver nanoparticle.⁷⁰ AgNO₃(5ml) solution was added to the leaf extract (1ml) and stirred at room temperature for 10 min develops reddish yellow color which is due to the formation of silver nanoparticles. UV absorption peak at 406 nm confirms the presence of silver NPs. The involvement of carbonyl group in the reduction of silver ion can be understood from IR spectral data. SEM results shows the polydispersity of nanoparticles and the strong EDX signal again confirms the presence of silver NPs along with oxygen, carbon peaks which may be due to the presence of terpenoids in the plant extract

Aqueous leaf extracts of *Azadirachta indica* was used for the synthesis of silver nanoparticle by Ikra.⁷¹ Optimization was carried out by varying concentration of both plant extract and silver ion concentration. Color change from yellowish to reddish brown due to the Surface Plasmon Resonance of silver particles and SPR were obtained at around 446nm. Spherical nature of silver nanoparticle was found out by TEM analysis and they also observed that there are some nanoparticles having irregular shape. Silver nanoparticle shows antibacterial activity against *E. coli* and *S. aureus*.

Arachis hypogaea peel extract was used for the synthesis of silver nanoparticles after 60min incubation at 28 °C.⁷² SPR appears at 450 nm and the increase in SPR accredited by increasing the incubation time. XRD pattern confirms the formation of fcc structured metallic silver. The nanoclusters are formed by the aggregation of nanoparticle which is evident from SEM images. The spherical nature of nanoparticle was identified from TEM images. Larvicidal activity of both extract and nanoparticle was studied against two important vector mosquitoes *A. stephensi* and *A. aegypti*. The synthesized silver nanoparticle was found to be better larvicidal agent compared to the extract.

Biosynthesis of silver nanoparticle was also carried out using palm date extract.⁷³ The reaction mixture was initially colorless and became yellow which then turns to bright brown on heating. Formation of silver nanoparticle was identified by SPR band at 425 nm. The nanoparticle forms a cluster by the aggregation of smaller silver nanoparticles. Palm date fruit extract derived silver nanoparticle shows better

antimicrobial activity compared to fruit extract alone. Catalytic activity of silver nanoparticle was studied for the reduction of 4-nitrophenol and observed that as the reaction time increases reduction efficiency increases.

Lemon peel extract was used for the reduction of silver ions to metallic silver at room temperature for 5 h.⁷⁴ The characteristic SPR band occurred at 420 nm and SEM analysis observed some spherical as well as irregularly shaped nanoparticle. Application of the biosynthesized nanoparticle was done against dermatophytes. They show better activity against *C. albicans* and *T. mentagrophytes*.

Silver nanoparticle with cubic shape was synthesized by the bioreduction of metal precursor using garlic clove extract and showed absorption at 408 nm. From XRD data the average size of nanoparticle was found to be 12 ± 2.3 nm which is in agreement with TEM results.⁷⁵ SEM images show the spherical nature of particles whereas EDX confirms the presence of silver. Cytotoxicity was studied against human lung epithelial (A549) and found that it not at all toxic at a concentration of 50 $\mu\text{g/ml}$.

Copper nanoparticles were synthesized from *Citrus medica* Linn using $\text{CuSO}_4\cdot 5\text{H}_2\text{O}$ by Rai and coworkers.⁷⁶ Addition of citron fruit extract to $\text{CuSO}_4\cdot 5\text{H}_2\text{O}$ followed by heating in the temperature range of 60-100 °C produces a visible color change from blue to pale yellow followed by deposition of reddish brown colored precipitates indicating the formation of copper NPs. This was collected and made a colloidal solution using liquid ammonia. SPR peak was observed at 631 nm. Size of the NPs was determined by NTA (Nanoparticle Tracking Analysis) based on the Brownian movement of the particles in the sample and the average range size was found to be 33 nm. XRD analysis proved that the copper has an fcc phase. They conducted *in vitro* antimicrobial activity against *E. coli*, *P. acne*, *K. pneumoniae*, *S. typhi*, and *P. aeruginosa* and three plant pathogenic fungi viz. *F. oxysporum*, *F. graminearum* and *F. culmorum*. The nanoparticles had higher activity against *E. coli*. Liquid ammonia or copper sulfate alone doesn't have any significant activity towards these organisms. Hudlikar reported a room temperature synthesis of copper nanoparticle from *Calotropis procera*.⁷⁷ Size of nanoparticle was determined using HR-TEM and found out to be in the range of 5-30 nm. The XRD pattern suggests an fcc structure for

copper nanoparticle. EDAX analysis gives elemental signals at 1.00, 1.50, 2.70 and 8.00 keV corresponds to copper. FTIR spectrum consists of amide II, amide III, secondary amine, carboxylic acid, alcohol bands. Cytotoxicity of the latex stabilized nanoparticle was done and showed excellent activity.

Kim *et.al* synthesized copper nanoparticle from *Mangolia kobus* leaves.⁷⁸ The effect of temperature and leaf broth concentration was studied. UV-Visible analysis shows absorption maximum at 560 nm. At 25 °C the conversion was about 70% whereas after 24 h this gradually increased to 100% at 90 °C. The particle size decreases from 110 nm obtained at 25 °C to 45 nm at 95 °C. As the reaction temperature increases the rate of the reaction as well as conversion of copper ion to copper nanoparticle increases. Influence of leaf broth concentration was investigated and the results showed that rate of reaction found to be highest at 20% concentration. The average particle size was found be decreased to 15% of leaf broth concentration and then increased. Both EDS and XPS results confirm the presence of copper nanoparticle. They compared the antibacterial activity of both biosynthesized copper nanoparticles with chemically synthesized one and found to be higher in the case of biosynthesized copper nanoparticles.

Catalytic application of copper nanoparticle derived from *Ginkgo biloba* leaf extract was reported by Nasrollahzadeh.⁷⁹ Nanoparticle were synthesized by mixing aqueous extract of leaves with $\text{CuCl}_2 \cdot 2\text{H}_2\text{O}$ solution followed by heating at 80 °C. The nanoparticles were collected by centrifugation followed by washing with n-hexane and ethanol. UV-visible spectrum shows absorption maxima in the range of 560-580 nm indicating the formation of copper nanoparticles. The average particle size was about 15-20 nm specified by TEM analysis. The catalytic activity of the synthesized copper nanoparticle was studied in azide-alkyne cycloaddition reaction. Optimization studies were carried out using benzyl chloride and phenyl acetylene. Ethanol was found to be good solvent and the use of 10 mol% of copper catalyst loading provides good result without any need of additional ligand or additives. Scope of the catalyst was studied using different alkynes and halides in ethanol at room temperature and good result were obtained. The product was recovered using centrifugation and washed with ethanol. The catalyst could be used as heterogeneous catalyst and reused four times without any significant loss in catalytic activity.

Nasrollahzadeh studied the Ullmann coupling reaction catalyzed by copper nanoparticle derived from leaf extract of *Euphorbia esula L.*⁸⁰ The SPR band observed at 580 nm corresponds to the surface Plasmon resonance which occurs due to the formation of copper nanoparticle. XRD diffraction pattern supports the formation of copper nanoparticles with fcc structure. Spherical shape of nanoparticle was identified by TEM analysis and it also shows the aggregation of smaller particle resulting in the formation of clusters. Reduction of 4-nitrophenol to 4-aminophenol was tested using the copper nanoparticle at room temperature in aqueous medium. The conversion to 4-aminophenol was monitored by UV-visible spectroscopy. To an aqueous solution of 4-nitrophenol NaBH₄ was added which produces 4-nitrophenolate ion having absorption at 403 nm. After the addition of copper nanoparticles, the phenolate absorption band disappeared and a new band formed at 300 nm which is the characteristic peak of 4-aminophenol. In order to optimize the reaction conditions, the reaction was carried out using different solvent and base. The best result was obtained when DMF used as solvent, Cs₂CO₃ as base and 1 ml of CuNP.

Copper nanoparticle was synthesized and stabilized using *Quisqualis indica* extract and evaluated its cytotoxic activity and apoptosis in B16F10 melanoma cells.⁸¹ Copper acetate was used as metal precursor and the addition of extract leads to the formation of copper nanoparticles. Synthesized copper nanoparticle was characterized by UV-vis spectroscopy which shows maximum absorption at 309 nm. Monodispersive and spherical nature of particles was observed by TEM analysis. The two theta values obtained corresponds to metallic copper further confirms the formation of copper nanoparticles.

Biosynthesis and application of copper nanoparticles in photocatalytic activity was studied by Bibi.⁸² Copper chloride on treatment with *P. grantam* seed extract at 70 °C was reduced to copper nanoparticle as indicated by the color change from dull bluish brown to dark green suspension. The precipitate was washed using water followed by ethanol and dried in a vacuum oven. Plasmon resonance was observed at 553nm. XRD pattern indexed to fcc structure of copper nanoparticles and EDX analysis confirms the presence of copper. The size of copper nanoparticles was found to be in 40-80 nm range. The copper nanoparticle shows excellent photocatalytic activity towards the methylene blue dye degradation.

Copper oxide nanoparticles were synthesized from *Punicagranatum* peels extract. To a solution of copper acetate the extract was added and stirred at room temperature.⁸³ Formation of copper oxide nanoparticle was indicated by the color change from blue to green color and its formation of brown suspension. SPR of copper oxide was observed at 282 nm and the formation was further confirmed by XRD analysis. The particle appears to be spherical in nature from SEM analysis .

Tabernaemontana divaricate mediated synthesis of copper oxide nanoparticles were reported by Sivaraj.⁸⁴ Aqueous solution of copper sulphate pentahydrate was treated with 50% leaf extract followed by stirring at 100 °C for 7-8 h resulted in a brownish black solid product. The antibacterial activity of copper oxide nanoparticle was studied using urinary tract pathogen and the highest zone of inhibition observed for *Escherichia coli*.

Application of biosynthesized copper nanoparticle towards the cyanation of aldehydes using $K_4Fe(CN)_6$ was studied by Nasrollahzadeh.⁸⁵ Reaction of $CuCl_2 \cdot 2H_2O$ with aqueous plant extract at 80 °C induces a color change which was the initial identification copper nanoparticle formation. The TEM image confirms the formation of nanosized copper particles in the range of 7-35 nm. The cyanation of aldehyde in the presence of copper nanoparticle afforded benzonitrile in 93% yield.

Scope of the work

Synthesis of nanoparticles using chemical or other methods stand with major drawback related to its separation from solvent and reaction mixture. “Green method” which uses natural source for the synthesis of nanoparticle reduces the use of toxic solvent and made the separation easier. Mace and seed of *Myrsitica fragrans* contains antioxidants, micronutrients and polyphenols which made it precious in medicinal field. The literature reports suggested the presence of phenyl propanoid ethers like eugenol in pericarp along with the same phytoconstituents found in the mace and seed. Pericarp of *myrsitica fragrans* doesn't gain much attention due to lack of knowledge about the medicinal values present in it. The fruit (pericarp) extract of *Myristica fragrans* alone can act as reducing as well as stabilizing agent in nanoparticle synthesis. Using the extract we had synthesized copper oxide nanoparticles and silver nanoparticle and investigated its catalytic and biological activities.

4.3.1 Reagents and Materials

- *Myrsitica fragrans* ripped fruit
- Copper acetate- Merck
- Silver Nitrate- Sigma Aldrich
- Benzyl chloride, 4-chlorobenzyl chloride, 2,4-dichlorobenzyl chloride, 4-nitro benzyl bromide, N-butyl bromide, allyl bromide, 1-chloromethyl naphthalene, cyclopentyl bromide and 2-bromoethyl benzene -Spectrochem Mumbai
- Sodium azide from Nice Chemicals
- Distilled water

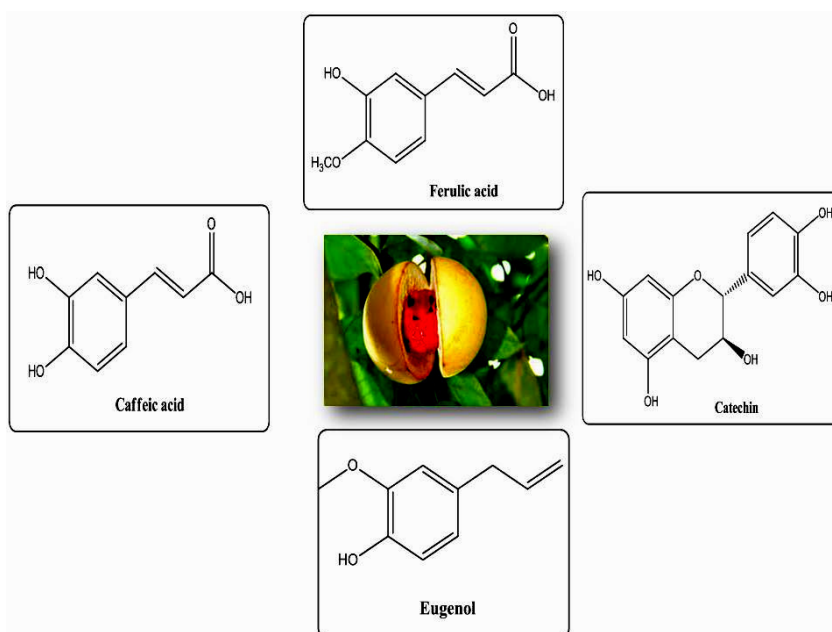
4.3.2 Instruments

- IR spectra recorded on a Shimadzu IR Affinity- 1 Spectrometer using KBr pellets
- SEM performed on JEOL Model JSM-7600F along with identification of chemical composition of sample using energy dispersive X-ray spectroscopy.
- NMR – Bruker Avance III, 400MHz
- GC-MS –Thermo Fisher Scientific
- TEM analysis done using Jeol/JEM 2100 instrument

4.4 Results and Discussion

The term biogenic synthesis is attributed to the use of biomaterials like plant parts, microorganisms *etc* for the synthesis and stabilization of metal ions to metal nanoparticles. To prepare nanoparticles, we used ripped fruit extract of *Myristica fragrans* which acts as both reducing and stabilizing agent. The genus *Myristica* belongs to the family Myristicaceae. In this genus the commonly found fruit is *Myristica fragrance*. It is commonly known as Nutmeg/ Javitri or Jaiphal, widely used as spice and ingredient in the Unnani, Ayurvedic medicine *etc.*^{86,87} The pericarp (fruit covering) is usually thrown away after taking the seed and arils surrounding the seed.

The reducing power of *Myristica fragrans* fruit extract is attributed to the presence of phytoconstituents present in the extract. Polyphenols, proteins *etc* influences the formation of metal nanoparticles.^{88,89} Earlier reports suggested the influence of phenolic acids such as caffeic acid, ferulic acid and catechin which is a flavanoid responsible for the formation of nanoparticles.^{90,91} Nutmeg contains phenylpropanoid ethers, acyl phenols, fatty acids, their esters, lignane, terpenes, phenolic acid and flavanoids.^{92,93} In addition to this, the preicarp of *Myristica fragran* contain phenyl propanoid ethers myristin, eugenol, isoeugenol and methyl eugenol. Among this, eugenol is the most predominant compound present in the pericarp of fruit, which promotes the reduction of metal ions to nanoparticle.⁹⁴



4.4.1 Preparation of *Myristica fragrans* fruit extract

The plant extract was prepared using hydrothermal method. Nutmeg fruit was dried under shade and powdered. Powdered Nutmeg fruit was mixed with distilled water in an autoclave and heated at 110 °C for 2 h. It was then allowed to cool into room temperature. The yellowish colored solution was filtered through Whatman no.1 filter paper and stored at 4 °C.

4.4.2 Visual Inspection

Freshly prepared copper acetate was irradiated under microwave in presence of *Myristica fragrans* fruit extract. The color of the copper acetate solution changes to bluish green and then to a greenish brown suspension indicating the formation of copper oxide (**Fig 1**). Further irradiation results in a black colored residue. The residue was separated by centrifugation and dried in a vacuum oven at 60 °C and used for further analysis.

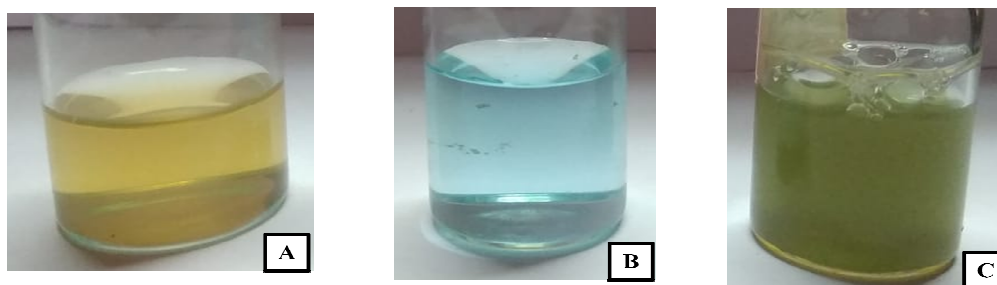


Fig 1 Photographs of A) *Myristica fragrans* fruit extract B) Copper acetate solution C) Reaction mixture containing CuO nanoparticles obtained after microwave irradiation

4.4.3 UV- Visible spectroscopy Analysis

A gradual color change of copper acetate solution from blue to bluish green then to greenish brown suspension after the addition of *Myristica fragrans* fruit extract is due to the formation of CuO nanoparticle. We observed the characteristic surface plasmon resonance of nano CuO and the corresponding band appears at λ 360 nm in the UV-visible spectrum (**Fig.2**)

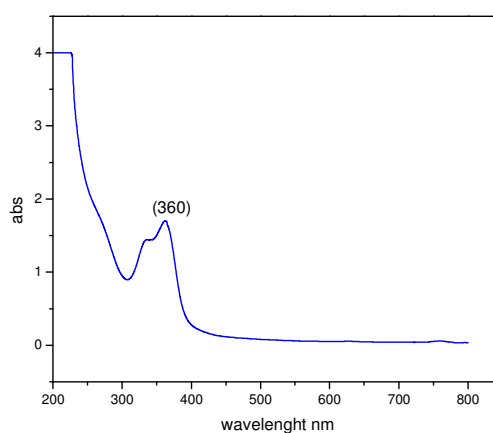


Fig 2. UV-Vis absorption spectrum of CuO nanoparticles

4.4.4 Infrared Spectral analysis

Fourier Transform Infrared (FTIR) analysis helps to identify the phytoconstituents present in the plant extract. FT IR of as synthesized CuONPs is shown in **Fig 3**. Characteristic Metal-oxide stretching vibration of CuO was observed at 497, 689 and 868 cm^{-1} and thereby confirms the presence of CuO in the sample. The presence of eugenol in sample was identified by observing characteristic IR peaks at 713 cm^{-1} and 1384 cm^{-1} corresponds to alkanes and alkane $\text{C-H}_{\text{rocking}}$ vibrations. Peak at 975 cm^{-1} observed for trans =C-H bond and 3238 cm^{-1} for phenolic -OH group. Aromatic ring -C=C stretching vibration was observed at 1556 cm^{-1} . From FT-IR analysis presence of both metal oxide and phytoconstituent which is responsible for the nanoparticle formation was confirmed.

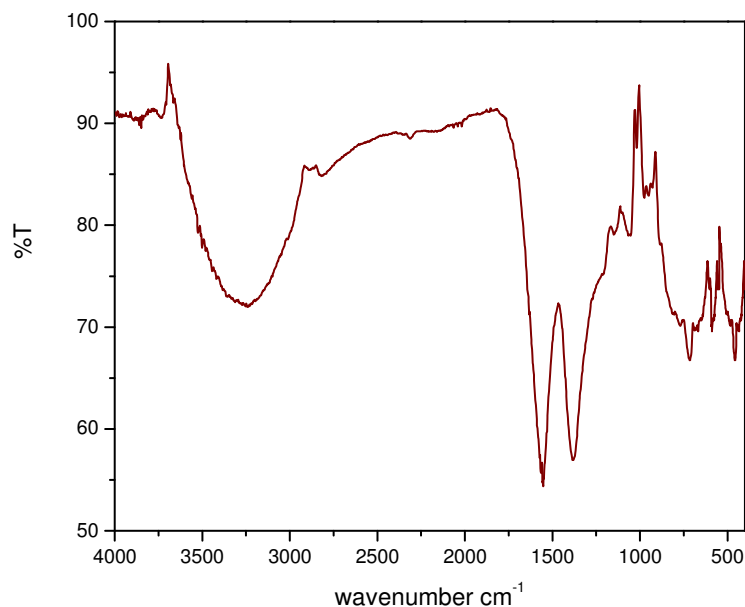


Fig 3 FT-IR Spectrum of CuO nanoparticle

4.4.5 Powder X-ray Diffraction Analysis

The XRD pattern (**Fig 4**) reveals the presence of CuO as the major component. The peaks at 2θ values of 32.5° , 35.6° , 38.8° , 48.7° , 50.5° , 58.4° , 61.5° , 66.4° , 67.9° , 73.7° corresponds to (1 1 0) (1 1 -1), (1 1 1), (2 0 -2), (1 1 2), (2 0 2), (1 1 -3), (3 1 0), (1 1 3), (2 2 1) planes of CuO monoclinic phase (JCPDS No:98-009-2367). Those peaks at 2θ values 29.7° , 42.4° corresponding to (0 1 1), (0 0 2), planes of Cu_2O (JCPDS No: 96-900-5770). 43.5° are attributed to (1 1 1) plane of Cu respectively ((JCPDS No. 04-0836)). The existence of copper(II)oxide was confirmed by XRD analysis with small amount of copper(I) oxide and copper(0) as impurities as a result of the over reduction of CuO by the plant extract.

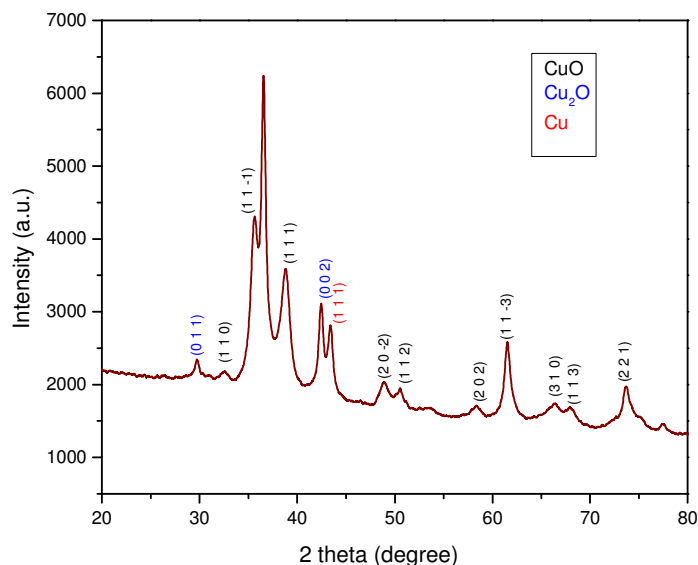


Fig. 4 XRD pattern of CuO nanoparticle -*Myristica fragrans* fruit extract

In vapor-solid method of nanowire synthesis, it is assumed that initial oxidation of copper acetate leads to the formation of Cu_2O and finally CuO was formed.⁹⁵ In certain cases complete reduction may occur resulting in metallic copper. The nanoparticle is considered to be an agglomeration of two or more individual crystallites. Using Debye-Scherrer equation the average crystallite size of the synthesized copper oxide nanoparticle was calculated.

$$D = \frac{K\lambda}{\beta \cos \theta}$$

Where

D= Crystallite size of copper oxide nanoparticle

K= The Scherrer constant with value from 0.9 to 1

λ = Wavelength of X-ray source used in XRD 0.15406 nm

β = full width at half maximum of the diffraction peak

θ = Bragg's angle

From the Scherrer equation the average crystallite size of copper oxide nanoparticle was found to be 15.7 nm.

4.4.6 Field emission gun scanning electron microscopy (FEG-SEM) Analysis

Typical SEM images of the synthesized CuO nanoparticles are shown in **Fig 5**. The SEM micrograph shows polydispersed spherically shaped particles embedded in the phytoconstituents. Using histogram average estimated particle size was found to be 13 ± 0.63 nm (**Fig. 5**)

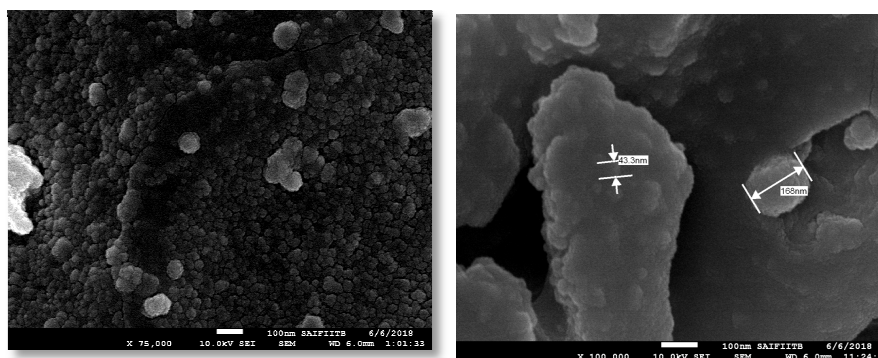


Fig. 5 Scanning electron microscopy(FEG-SEM) images of CuO nanoparticle synthesized using *Myristica fragrans* fruit extract

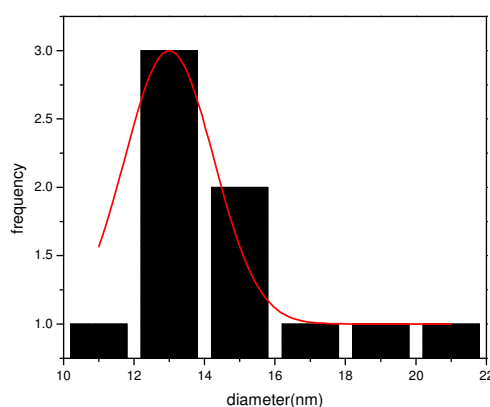


Fig.6 Particle size distribution histogram of CuO nanoparticles

Energy Dispersive X-ray Spectroscopy (EDS) Analysis

The elemental composition of CuO nanoparticle was determined by energy dispersive X-ray spectroscopy (EDS) and shown in **Fig 6**. This spectrum shows a high intense peak at 0.9 and the less intense peak at 8.1 and 8.9 keV represents $\text{CuL}\alpha$, $\text{CuK}\alpha$ and $\text{CuK}\beta$ respectively with wt% of 44.11% and a strong peak for elemental oxygen at 0.5keV with wt% of 33.64% which confirms the formation of CuO. Signals obtained

for Na, K, Ca and Zn which can be due to the existence of biomolecules around the nanoparticles.

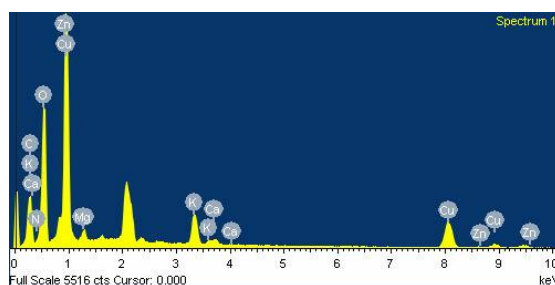


Fig 7 EDS spectrum of CuO NPs-*Myristica fragrans* fruit extract

4.4.7 High resolution transmission electron microscopy (HR-TEM) analysis

The HR-TEM confirms the formation spherical shaped copper oxide nanoparticle which is surrounded by plant biomass. (Fig.7 A,B &C).

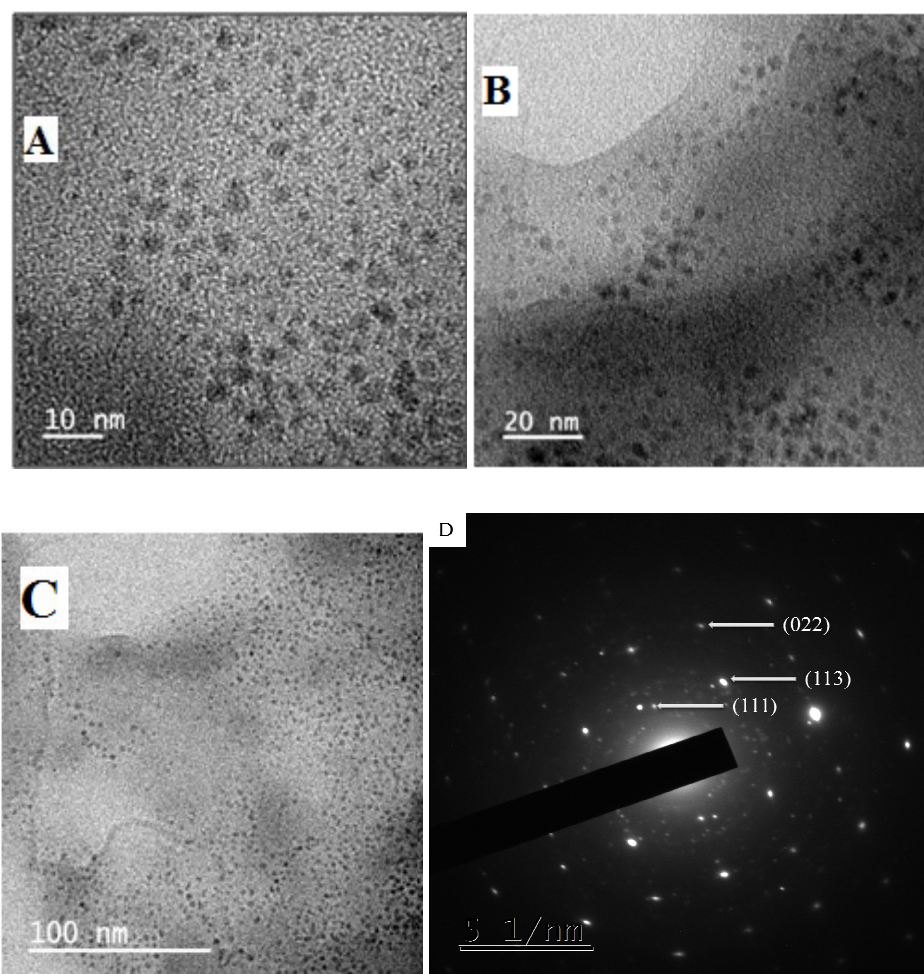
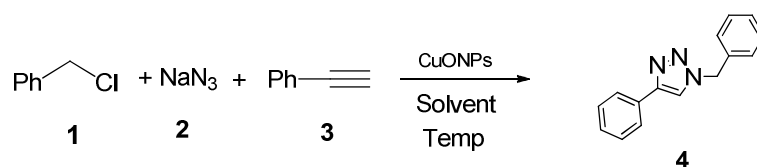


Fig 8 HR-TEM images of CuO NPs at different different magnification (A,B &C) and SAED pattern (D)

The SAED pattern (**Fig 7D**) has the nature of sharp rings with small spots indicating that the compound is nanocrystalline in nature. The “d” spacing was estimated to be 0.21, 0.13, 0.10 nm and that corresponds to “d” spacing of the (111), (113) and (022) orientation of monoclinic structure of metallic CuO nanoparticle.

4.4.8 Catalytic Activity of the Synthesized Copper oxide (CuO) nanoparticle in Azide-Alkyne Cycloaddition reaction

After the successful synthesis and characterization of CuO nanoparticle its catalytic activity was studied for the synthesis of 1,2,3-triazoles using phenyl acetylene, sodium azide and alky/aryl halides. Optimization studies were carried out using benzyl chloride, phenyl acetylene and sodium azide as reactants in terms of solvent, catalyst loading, temperature (**Scheme 1**). The optimization results (**Table 1**) show the effect of solvent on the product yield. Water, ethanol, THF and ethanol/water mixture were tested. Among these solvents water shows a remarkable effect on triazole formation. The best result obtained when 0.01 g of CuO nanoparticle in water at 60 °C (**Table 1, entry 6**). The product was separated by extraction using ethyl acetate and the insoluble catalyst was recovered and dried in vacuum oven at 70 °C. The recyclability of the catalyst was studied using the model reaction and the recovered catalyst was used for a new set of reactions. No significant loss in catalytic activity was observed after the successive first four runs. The CuO nanoparticle could be reused as heterogeneous catalyst. By increasing the catalyst concentration to 0.02 g, the reaction completed within 4 h. Using optimized conditions triazoles with different functional groups have been synthesized from corresponding alkyl/aryl halides and alkynes (**Table 2**).

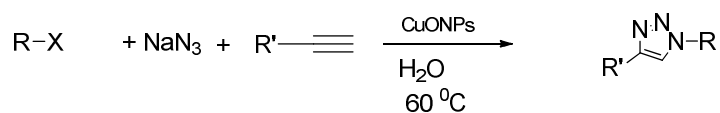


Scheme 1

Table 1 Optimization of the CuAAC reaction in terms of catalyst loading, solvent, temperature and time using benzyl chloride, sodium azide, phenyl acetylene and CuO NPs

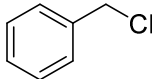
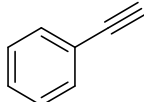
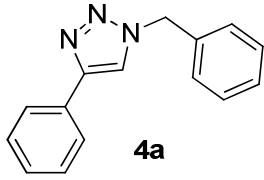
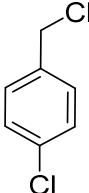
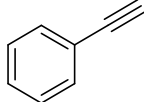
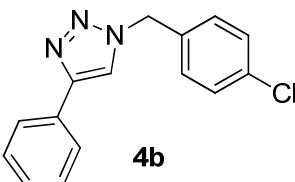
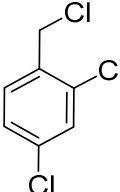
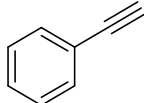
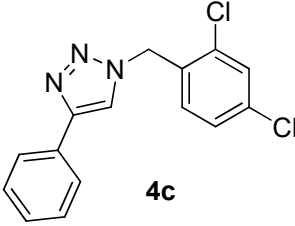
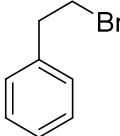
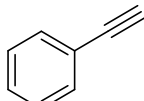
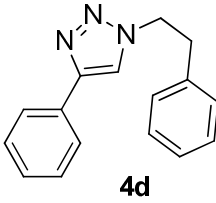
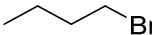
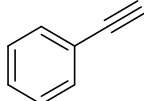
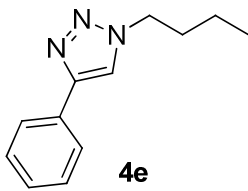
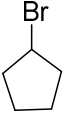
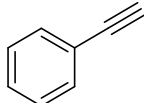
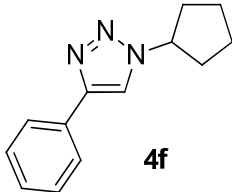
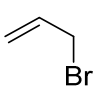
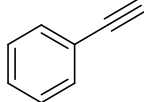
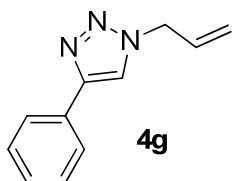
Entry	Catalyst loading(g)	Solvent	Temperature	Time(h)	Yield %
1	0.01	H ₂ O	rt	12	70
2	0.01	Ethanol	rt	48	65
3	0.01	THF	rt	48	Nil
4	0.01	t-BuOH	rt	20	75
5	0.01	Ethanol/H ₂ O	rt	20	50
6	0.01	H ₂ O	60°C	5	98
7	0.01	Ethanol	60°C	5	70
8	0.005	H ₂ O	60°C	15	90
9	0.02	H ₂ O	60°C	4	98

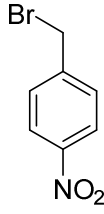
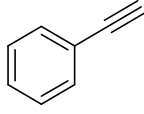
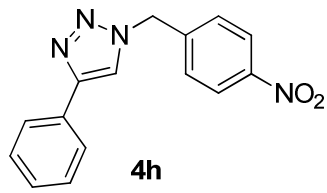
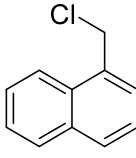
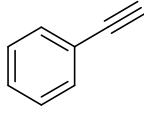
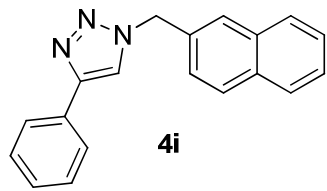
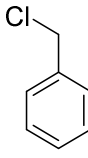
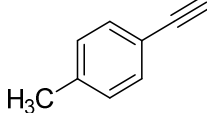
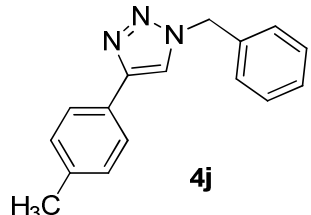
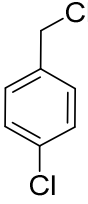
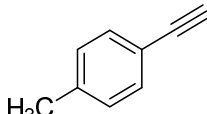
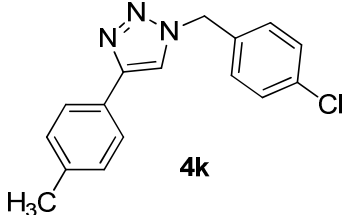
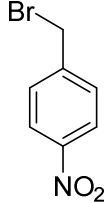
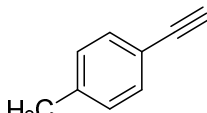
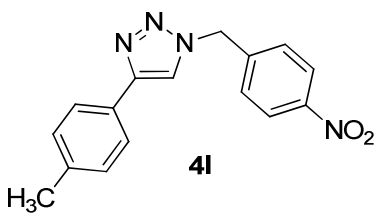
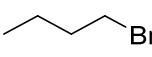
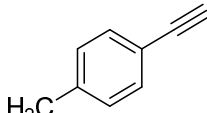
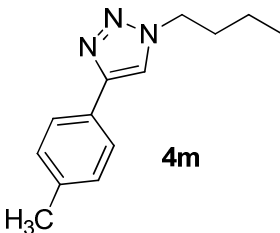
Reaction conditions: benzyl chloride(1 mmol), NaN₃ (1.5 mmol), phenyl acetylene (2 mmol) and solvent (5 ml)



Scheme 2

Table 2 Synthesis of 1,4-disubstituted 1,2,3-triazole using alkyl/aryl halides and alkyne

Sl No.	RX	R'	Product	Yield
1			 4a	98
2			 4b	95
3			 4c	91
4			 4d	98
5			 4e	85
6			 4f	80
7			 4g	90

8			 4h	97
9			 4i	90
10			 4j	92
11			 4k	90
12			 4l	91
13			 4m	84

Reaction conditions: organic halide(1 mmol), NaN₃ (1.5 mmol), alkyne (2 mmol) and CuONPs (10 mg) in water (5 ml) at 60 °C for 5h

Substituents present on both azide and alkyne shows a little effect in the overall yield of products. Among the electron withdrawing substituents Cl⁻ and NO₂, chlorine possess much more effect on decreasing the yield of the reaction (**Table 2, entry 2, 3 & 11**). A drastic decrease in the yield was observed as the azide

changes from aryl to alkyl (**Table 2, entry 5, 6 & 11**). Presence of substituent on alkyne also influences the reaction. Electron releasing substituent decreases the yield (**Table 2, entry 10, 11, 12 & 13**).

Reusability of the catalyst was also studied using the same model reaction under same reaction conditions. Insolubility of CuO in water made the easy recovery of the catalyst by simple filtration. Organic impurities which may present in the surface of catalyst were removed by washing with water and acetone followed by drying in vacuum oven at 70 °C for 3 h. Recovered catalyst can be reused four times with slight decrease in the yield (**Table 3, Fig 9**).

Table 3 Reusability of CuO NPs

	Yield (%)
Native	98
1	95
2	91
3	90
4	87

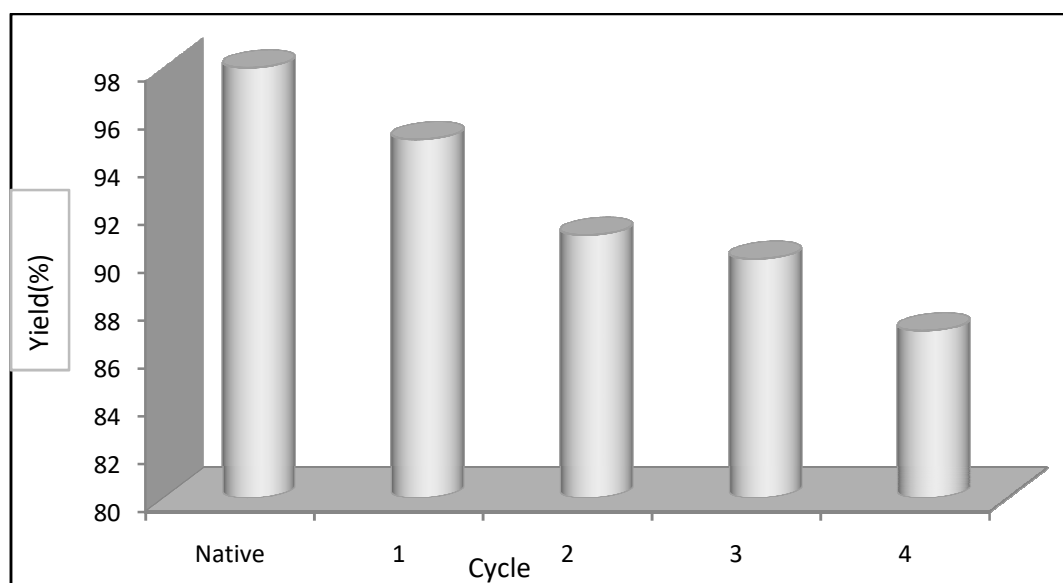
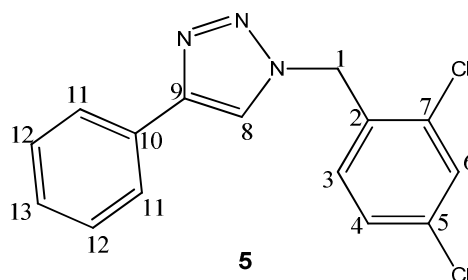


Fig 9 Reusability of CuO NPs in CuAAC reaction

4.4.9 Characterization of 1,4-disubstituted 1,2,3-triazoles

For the general discussion, the compound 1-(2,4-dichlorobenzyl)-4-phenyl-1H-1,2,3-triazole **5** was taken as a representative molecule.



The FT-IR spectrum (**Fig 10**) of the compound gives major absorptions at 1452, 1209, 839 cm^{-1} corresponds to $-\text{CH}_2$, $\text{N}=\text{N}=\text{N}$ - and $=\text{C}-\text{H}$ stretching of triazole ring.

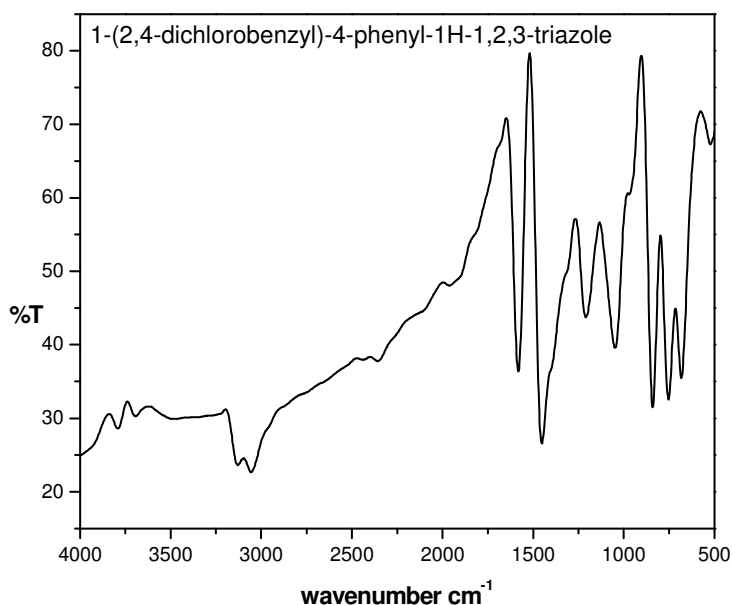


Fig 10 FTIR spectrum of 1-(2,4-dichlorobenzyl)-4-phenyl-1H-1,2,3-triazole

Structure of the triazole was further confirmed by ^1H NMR spectrum (**Fig. 11**). The $-\text{CH}_2$ proton of benzyl is observed as two proton singlet at δ 5.70. Proton at C3 (3) gives a doublet at δ 7.49, whereas proton at C4 provide peak at δ 7.20 and at C6 provides doublet at δ 7.36. The characteristic $=\text{C}-\text{H}$ proton at C8 and ortho phenylic

proton at C11 provide triplet at δ 7.83. Meta protons at C12 of phenyl group gives peak at δ 7.43 and the C13 para proton at δ 7.28.

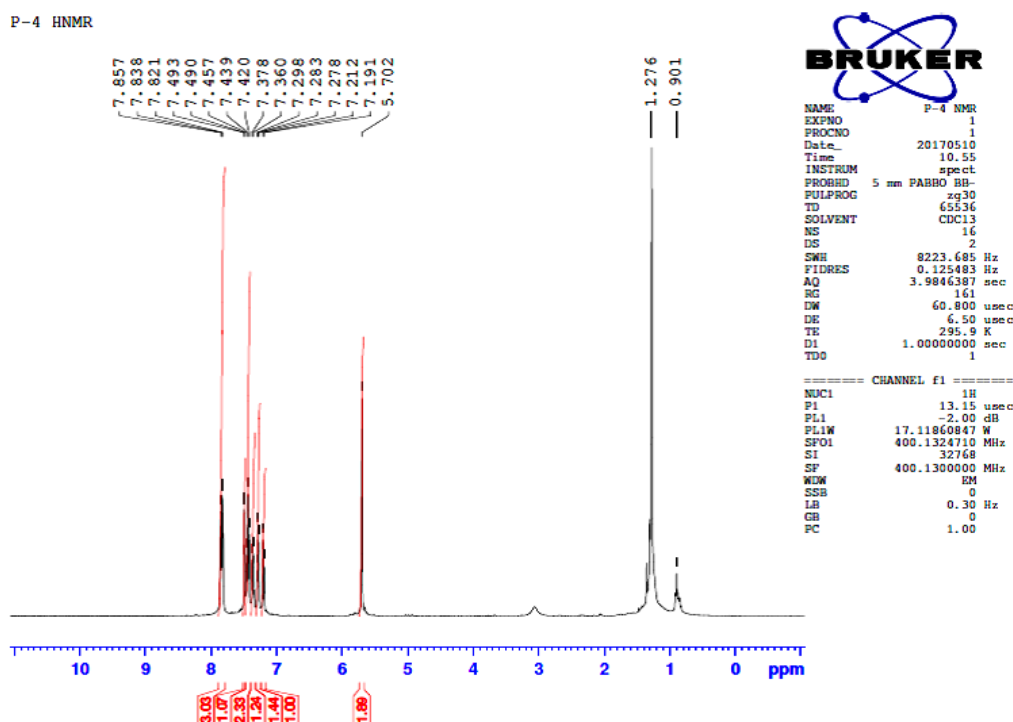


Fig. 11 ^1H NMR spectrum of 1-(2,4-dichlorobenzyl)-4-phenyl-1H-1,2,3-triazole

The ^{13}C NMR spectrum (**Fig 12**) is in agreement with both ^1H NMR and FT-IR data. The downfield peak at δ 148.0 is due to the carbon at the position 9. The characteristic peak of triazole carbon (C8) that is directly bonded to hydrogen was observed at δ 119.9 confirms the formation 1,4-disubstituted triazoles.⁹⁶ The benzylic carbon C1 gives peak at δ 51.9 and the values at 135.7, 128.0, 128.5, and 134.1, 134.1 attributed to the phenyl carbons C2, C3, C4, C5 and C7 carbons. Both C6 and C10 show peak at δ 129.85. Other peaks at 125.8, 128.7 and 128.9 are respectively the ortho, meta and para carbons of phenyl ring.

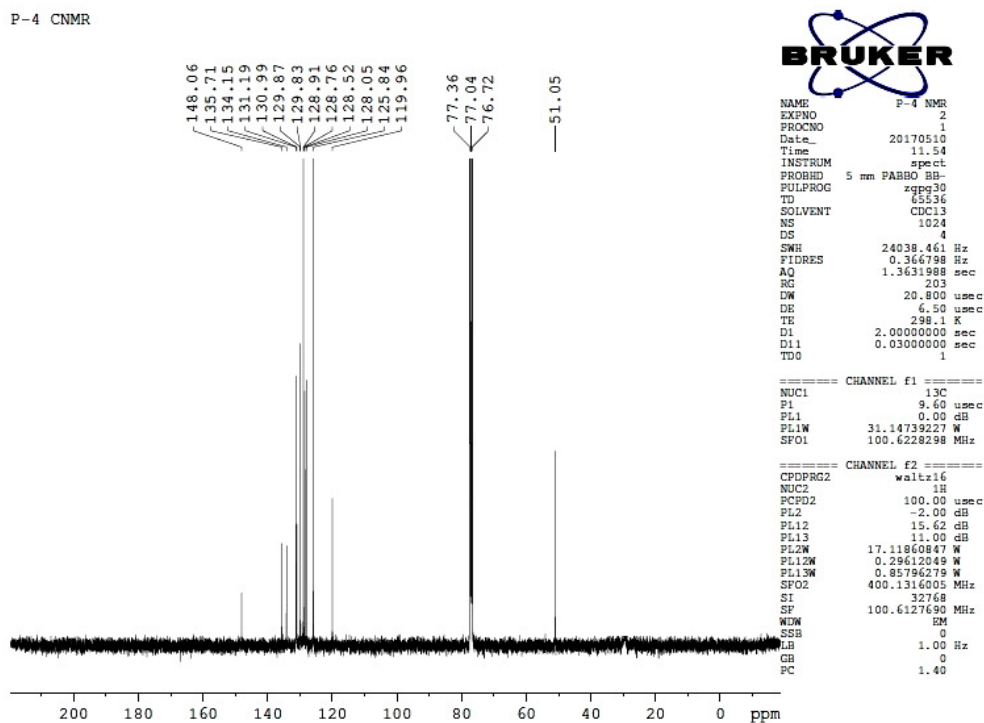


Fig. 12 ^{13}C NMR spectrum of 1-(2,4-dichlorobenzyl)-4-phenyl-1H-1,2,3-triazole

The structure of the compound was further confirmed by mass spectral analysis. The molecular ion peak (M^+) observed at m/z 303 (10), 307.03 ($M+4$), 116 ($M-\text{C}_7\text{H}_6\text{Cl}_2\text{N}_2$) (**Fig. 13**).

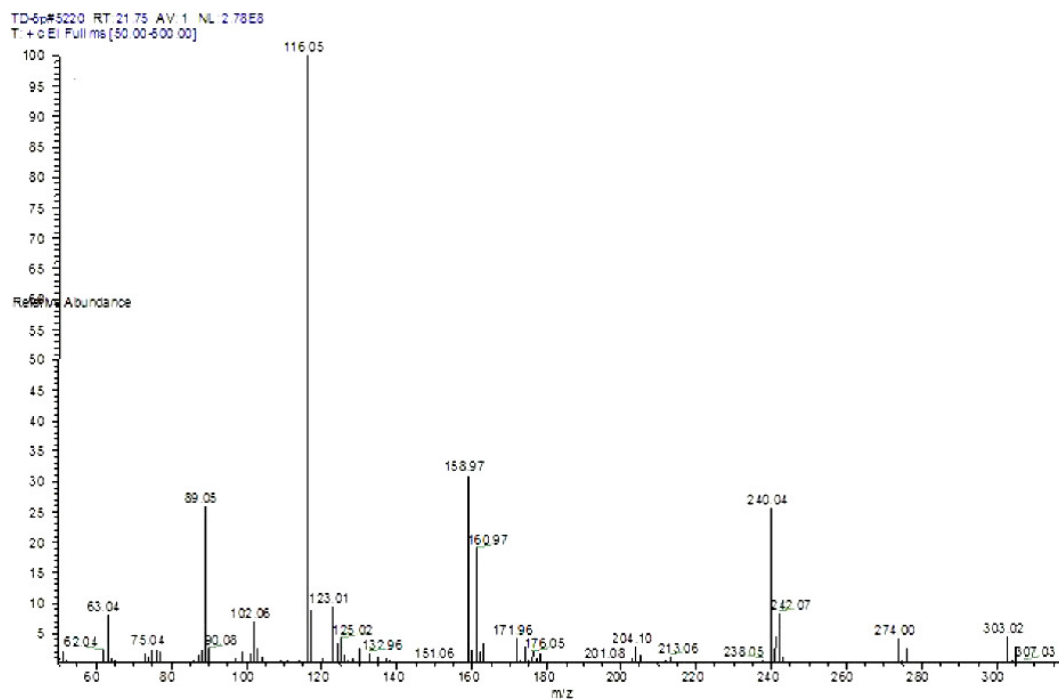
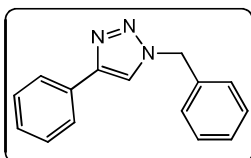


Fig 13 Mass spectrum of 1-(2,4-dichlorobenzyl)-4-phenyl-1H-1,2,3-triazole

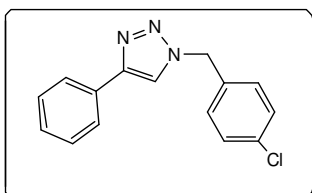
4.5 Spectral data of 1,4-disubstituted 1,2,3,-triazoles

1. 1-Benzyl-4-phenyl-1*H*-1,2,3-triazole (4a)



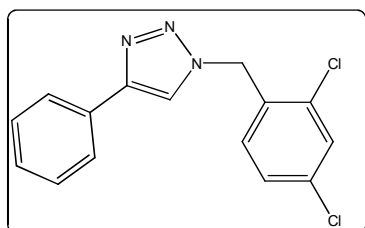
^1H NMR (400 MHz, CDCl_3): δ 5.29(s,2H), 7.18(d,2H, $J=7.2\text{Hz}$), 7.30(t,1H), 7.38 (m, 2H), 7.42(t,1H), 7.64(s,1H), 7.66(dd,2H), 7.44(m,2H). ^{13}C NMR (100.6 MHz, CDCl_3): δ 52.7, 119.4, 125.7, 127.8, 128.6, 128.7, 128.9, 128.9, 129.1, 135.1, 147.3. Mass m/z (%): 235.08 (M^+). FTIR (KBr): 3110, 3100, 3052, 3020, 2950, 1492, 1462, 1420, 1343, 1220, 1180, 1070, 1085, 1020, 940, 825, 810, 757, 690, 475 cm^{-1}

2. 1-(4-chlorobenzyl)-4-phenyl-1*H*-1,2,3-triazole (4b)



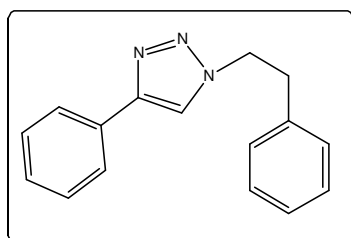
^1H NMR (400 MHz, CDCl_3): δ 5.45(s,2H), 7.18(d,3H, $J=7.2\text{Hz}$), 7.36-7.28(m,6H), 7.78(s,1H). ^{13}C NMR (100.6 MHz, CDCl_3): δ 51.2, 119.4, 125.2, 128, 128.6, 129.5, 130.9, 132.4, 133.8, 135, 149.2. Mass m/z (%): 269 (M^+ , 10), 271 (M^++2 , 4), 116 (100), 125(44). FTIR (KBr): 3107, 3082, 3064, 3034, 2933, 1492, 1462, 1411, 1350, 1220, 1143, 1091, 1080, 1016, 975, 819, 804, 763, 688, 495 cm^{-1}

3. 1-(2,4-dichlorobenzyl)-4-phenyl-1*H*-1,2,3-triazole (4c)



^1H NMR (400MHz, CDCl_3) δ : 5.67 (s 2H), 7.16 (s, 1H), 7.25–7.46 (m, 4H), 7.88 (s, 3H). ^{13}C NMR (100.6MHz, CDCl_3) δ : 50.8, 119.8, 125.7, 127.9, 128.2, 128.8, 129.7, 130.3, 131, 131.3, 134.1, 135.5, 148.2; Mass m/z (%): 303 (M^+ , 5), 305 (M^++2 , 3), 240, 158, 116 (100).

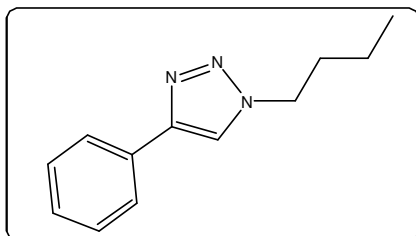
4. 4-phenyl- 1-(2-phenylethyl)-1*H*-1,2,3-triazole (4d)



^1H NMR (400 MHz, CDCl_3): δ 3.30 (t, 2H, $J = 7.2\text{Hz}$), 4.71 (t, 2H, $J = 7.6\text{Hz}$), 7.20 (d, 1H, $J=6.8$), 7.30–7.36 (m, 3H), 7.42 (t, 2H, $J = 7.2\text{Hz}$), 7.50 (s, 1H), 7.81 (d, 2H, $J = 6.8\text{Hz}$). ^{13}C NMR (100.6 MHz, CDCl_3) δ : 52.7, 37.3, 120.1, 122.0, 125.7, 127.5, 128.2, 128.7, 128.8, 131.7, 137.5, 148.2.

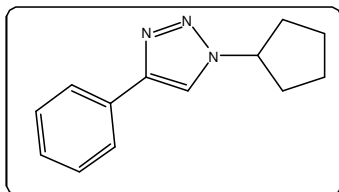
Mass m/z (%): 249 (M^+ , 35), 220 (18), 193 (13), 179 (8), 130 (34), 118 (71), 105(100), 77 (42), 51 (8). FTIR (KBr): 3107, 3028, 1683, 1483, 1450, 1365, 1220, 1080, 1043, 94, 910, 844, 734, 690 cm^{-1}

5. 1-Butyl-4-phenyl-1H-1,2,3-triazole (4e)



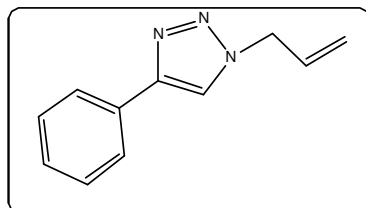
^1H NMR (400 MHz, CDCl_3): δ 0.98(t, 3H, $J = 7.2\text{Hz}$), 1.40–1.46 (m, 2H), 1.80–1.85(m, 2H), 4.60(t, 2H, $J = 7.2\text{Hz}$), 7.40(d, 1H, $J=7.2\text{Hz}$) 7.51(t, 2H, $J=7.2\text{Hz}$), 7.80 (s, 1H), 7.89 (d, 2H, $J=7.2\text{Hz}$). ^{13}C NMR (100.6MHz, CDCl_3): δ 12.9, 20.2, 31.9, 50.5, 119.6, 125, 128.8, 129.2, 131.2, 148.2. Mass m/z (%): 201 (M^+ , 33), 145 (16), 117 (100), 90 (24). FTIR (KBr): 3062, 2947, 2870, 1460, 1367, 1215, 1066, 761, 692 cm^{-1}

6. 1-cyclopentyl-4-phenyl-1H-1,2,3-triazole (4f)

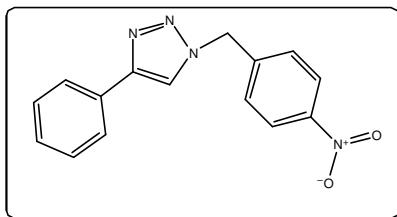


^1H NMR (400 MHz, CDCl_3): δ 1.76–1.7 (m, 2H), 1.91–1.95 (m, 2H), 2.05–2.12 (m, 2H), 2.26–2.31 (m, 2H), 4.94–5.01 (m, 1H), 7.31 (t, 1H, $J = 7.2\text{Hz}$), 7.39 (m, 2H), 7.82 (s, 1H), 7.83 (dd, 2H, $J=7.7, 1.55$). ^{13}C NMR (100.6 MHz, CDCl_3): δ 23.6, 32.1, 58.8, 119, 125.7, 128.0, 128.7, 129.1, 147.3. Mass m/z (%): 213 (M^+ 33), 184, 156, 117 (100).

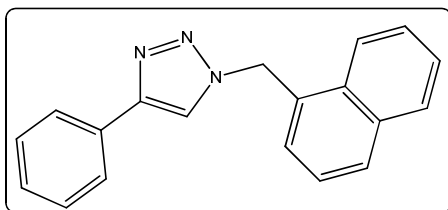
7. 1-allyl-4-phenyl-1H-1,2,3-triazole (4g)



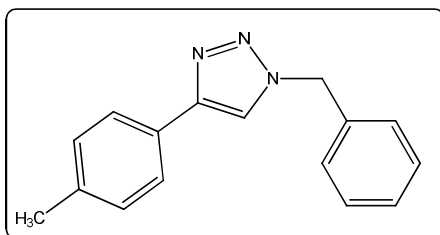
^1H NMR (400 MHz, CDCl_3): δ 5.02(dd, 1H, $J = 16.4\text{Hz}$), 5.36(dd, 1H, $J= 10\text{Hz}$), 6.01–6.11 (m, 1H), 7.31–7.44 (m, 3H), 7.76 (s, 1H), 7.83(d, 2H, $J = 7.6\text{Hz}$). ^{13}C NMR(100.6MHz, CDCl_3): δ 47.6, 7, 117.6, 120.2, 125.7, 128.7, 128.9, 129.1, 131.3, 147.3. Mass m/z (%): 185(M^+ , 19), 116(100). FTIR (KBr): 3120, 3088, 2934, 2854, 1645, 1608, 1460, 1334, 1219, 1166, 1049. 985, 914, 825, 765, 690, 509 cm^{-1}

8. 1-(4-Nitrobenzyl)-4-phenyl-1H-1,2,3-triazole (4h)

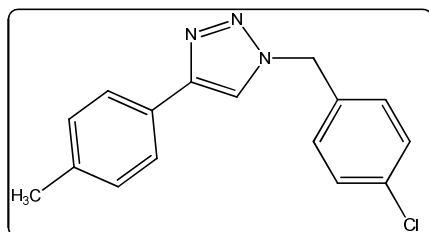
^1H NMR (400 MHz, CDCl_3): δ 5.69 (s, 2H), 7.34-7.45(m,5H), 7.76(s, 1H), 7.80(d, 2H, $J = 7.6\text{Hz}$), 8.22(d, 2H, $J = 8\text{Hz}$). ^{13}C NMR (100.6MHz, CDCl_3): δ 52.7, 119.7, 124.3, 125.7, 128.5, 128.9,129.1, 135, 140.5, 147.3. Mass, m/z (%): 281 (M^+ , 19), 207 (44), 116 (100), 106 (24), 89 (43). FTIR (KBr): 3118, 3080, 2939, 2857, 1600, 1517, 1429, 1346, 1209, 1107, 1074, 1305, 844, 815, 761, 729, 686 cm^{-1}

9. 1-(naphthyl)-4-phenyl-1H-1,2,3-triazole (4i)

^1H NMR (400 MHz, CDCl_3): δ 5.91(s, 2H), 7.37-7.44 (m, 5H), 7.65 (m, 2H),7.81 (m, 2H), 7.90 (m, 3H) 7.91 (s, 1H). ^{13}C NMR (100.6MHz, CDCl_3): δ 55.3,119.7, 124.2, 125.6, 125.8, 126.5, 126.9, 127.5, 128.2, 129.3, 129.7, 130.1, 132.6, 133.5, 133.9, 134.0,. Mass m/z (%): 284 (M^+ , 5), 253 (10), 207 (98), 115 (90), 84(100). FTIR (KBr); 3115, 2924, 2848, 1454, 1431, 1344, 1307, 1211, 114, 1080, 1037, 974, 912, 842, 771, 688 cm^{-1}

10. 1-(benzyl)-4(p-tolyl)-1H-1,2,3-triazole (4j)

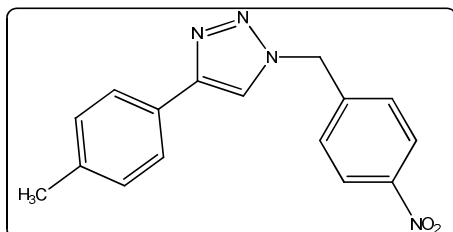
^1H NMR (400 MHz, CDCl_3): δ 2.38 (s, 3H), 5.58 (s, 2H), 7.22 (d, 2H, $J = 7.6\text{Hz}$), 7.32-7.41(m, 5H), 7.66 (1H, s), 7.71 (d, 2H, $J = 8.4\text{Hz}$). ^{13}C NMR (100.6MHz, CDCl_3): δ 148.14, 138.18, 134.62,129.52, 129.17, 128.82, 128.1, 127.41, 125.68, 54.33, 21.33. Mass m/z (%): 249(M^+ , 15), 220(63), 130(100), 91(72), 77(18) FTIR (KBr): 3138, 3008, 2902, 1446, 1342, 1213, 1122, 1045, 968, 788, 713, 584, 512 cm^{-1}

11. 1-(4-chlorobenzyl)-4-(p-tolyl)-1H-1,2,3-triazole (4k)

^1H NMR (400 MHz, CDCl_3): δ 2.38 (s, 3H), 5.55 (s, 2H), 7.22-7.28(m,3H) 7.37(d,2H, $J = 8.4\text{Hz}$), 7.67 (s, 1H), 7.71 (d, 2H, $J = 8\text{Hz}$) ^{13}C

NMR (100.6MHz, CDCl₃): δ 24.3, 57.0, 125.6, 127.4, 128.8, 129.6, 130.1, 131.3, 134.4, 138.4, 146.3. Mass m/z (%): 283 (M⁺, 12), 254 (35), 130(100). FTIR (KBr): 3113, 3012, 2953, 1485, 1436, 1334, 1207, 1080, 1033, 808, 750, 507 cm⁻¹

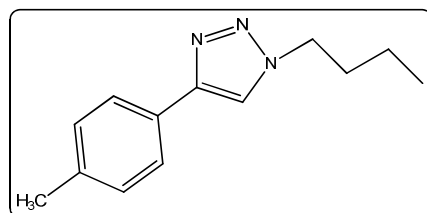
12. 1-(4-Nitrobenzyl)-4-(p-tolyl)-1H-1,2,3-triazole (4l)



¹H NMR (400 MHz, CDCl₃): δ 2.39 (s, 3H), 5.71 (s, 2H), 7.24 (d, 2H, $J = 7.6$ Hz), 7.46 (d, 2H, $J = 8.4$ Hz), 7.72 (d, 2H, $J = 8$ Hz), 7.77 (s, 1H) 8.24 (d, 2H, $J = 8.4$ Hz). ¹³C

NMR(100.6MHz, CDCl₃): δ 24.3, 57.0, 121.0, 125.7, 127.4, 129.6, 130.1, 138.4, 145.4, 146.3. Mass m/z (%): 294(M⁺ 9), 281 (25), 207 (70), 130 (100). FTIR (KBr): 3088, 3034. 2924, 2856, 1602, 1516, 1444, 1344, 1213, 1101, 1039, 972, 810, 723, 513 cm⁻¹

13. 1-Butyl-4-(p-tolyl)-1H-1,2,3-triazole (4m)



¹H NMR (400 MHz, CDCl₃): δ 0.89 (t, 3H, $J = 7.2$ Hz), 1.29-1.34 (m, 2H), 1.87 (m, 2H), 2.30 (t, 3H, $J = 6.4$ Hz), 4.34 (s, 3H), 7.06-7.18 (m,

3H), 7.33 (m, 2H), 7.73 (s, 1H). ¹³C NMR (100.6MHz, CDCl₃): δ 13.8, 20.3, 24.3, 30.6, 52.2, 119.7, 125.6, 127.5, 129.2, 130.1, 138.4. Mass m/z (%): 215 (M⁺, 40), 159(30), 144 (35), 131(100).

4.6 Sunlight induced rapid synthesis of silver nanoparticles

Sunlight is believed to be the largest natural, renewable energy source which is non-toxic and non-polluting. Earlier reports imply that, in nanoparticle synthesis sunlight act as catalyst in presence of reducing agents which is believed to cause photo-excitation process.⁹⁷⁻⁹⁹

4.6.1 Visual Inspection of silver nanoparticle

Myristica fragrans fruit extract was added to silver nitrate solution. In dark conditions, the color of the solution remains unchanged even after 24h. After the exposure to sunlight the color of the solution changes from yellow to brown within 10 min of incubation due to the formation of silver nanoparticle (**Fig 14**).

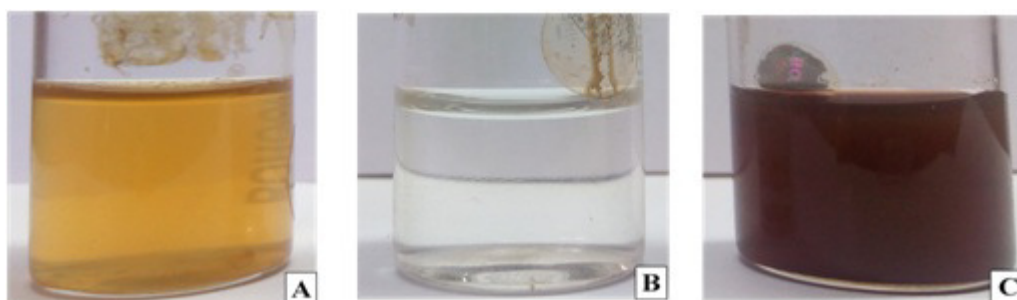


Fig 14 Photographs of A) *Myristica fragrans* fruit extract B) AgNO_3 solution C) Reaction mixture containing silver nanoparticle

4.6.2 UV-Visible spectral studies of silver nanoparticle

The gradual color change from yellow to brown is attributed to the reduction of Ag^+ to Ag^0 . The final brown color is due to the formation of silver nanoparticle which was due to the surface plasmon vibrations of the synthesized nanoparticle and the SPR band was observed at 478 nm (**Fig 15**). The emergence of surface plasmon resonance can be explained as follows; the metallic silver contains large number of conducting electron and the united oscillation of these conducting electrons results the excitation of local surface plasmon resonances leading to the strong light scattering by the electric field at wavelength of resonance occurred.⁶⁶ The difference in the absorption range depends on the size and shape of nanoparticle.

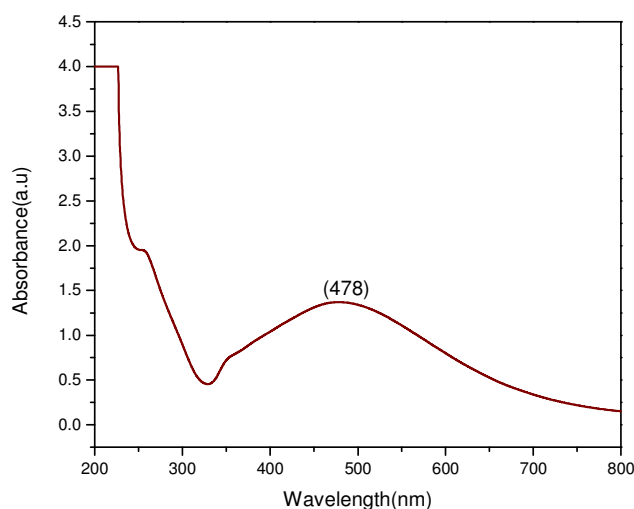


Fig. 15 UV- Visible spectrum of Ag NPs

4.6.3 Infrared Spectral studies

FT-IR spectrum of silver nanoparticle is given in **Fig 16**. It again confirms the presence of eugenol in the synthesized nanoparticle. Band at 673 and 744 cm^{-1} corresponds to aromatic-CH out of plane bending vibration. Bending vibration of =C-H was observed at both 906 and 909 cm^{-1} . C-O-C stretching vibration of ether was observed at 1026 cm^{-1} and that of $-\text{CH}_2$ bending observed at 1421 cm^{-1} . $-\text{C-H}$ stretching vibration was observed at 2843 and 2920 cm^{-1} and phenolic $-\text{OH}$ observed at 3244 cm^{-1} .

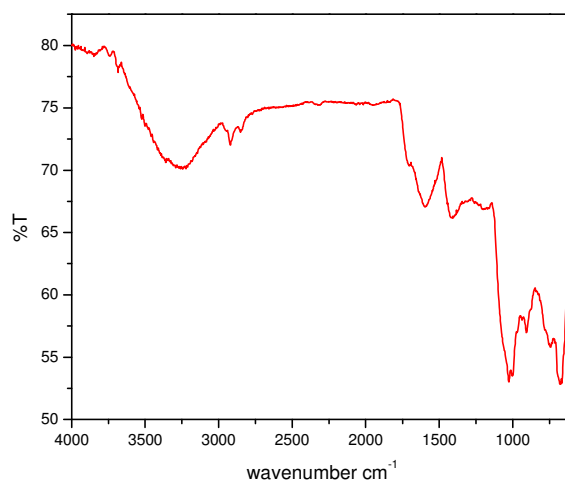


Fig. 16 FT-IR spectrum of Silver nanoparticle

4.6.4 Powder X-ray Diffraction Analysis

The diffractogram is as shown in **Fig 17**. From this formation of silver nanoparticle was confirmed. The two theta values at 38.4° , 44.6° , 64.8° , 77.6° corresponds to (1 1 1), (0 0 2), (0 2 2) and (1 1 3) reflection of face centered cubic silver crystal (JCPDS No: 00-004-0783). Due to longer exposure to atmospheric oxygen silver nanoparticle gets oxidized to silver oxide with two theta values 32.5° , 46.5° , 55.1° and 57.8° indexed as (1 1 1), (1 1 2), (0 2 2) and (1 2 2) planes of silver corresponds to cubic crystal structure (JCPDS No :98-017-4092).

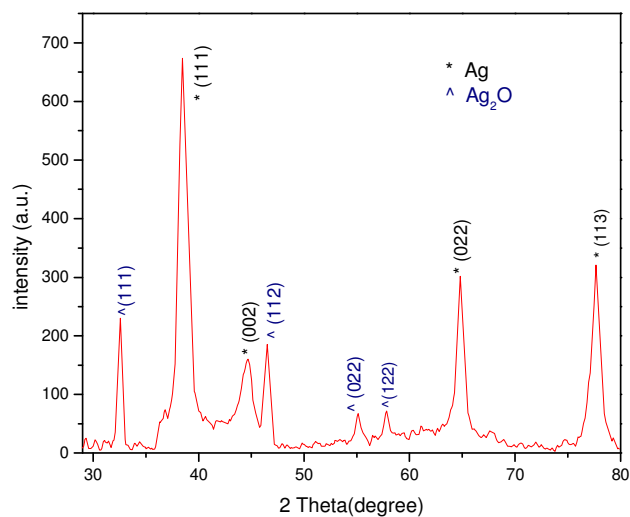


Fig. 17 XRD pattern of Ag NPs

4.6.5 Energy Dispersive X-ray Spectroscopy (EDS) Analysis

The EDX analysis provides both qualitative and quantitative information about elements involved in the formation of silver nanoparticle (**Fig 18**). The peak at 3keV due to silver with wt% of 32.7% confirms the presence of silver nanoparticle which may be attributed to their surface plasmon resonance¹⁰⁰. The elemental profile of other elements due to the existence of biomolecules and micronutrients associated with plant extract.

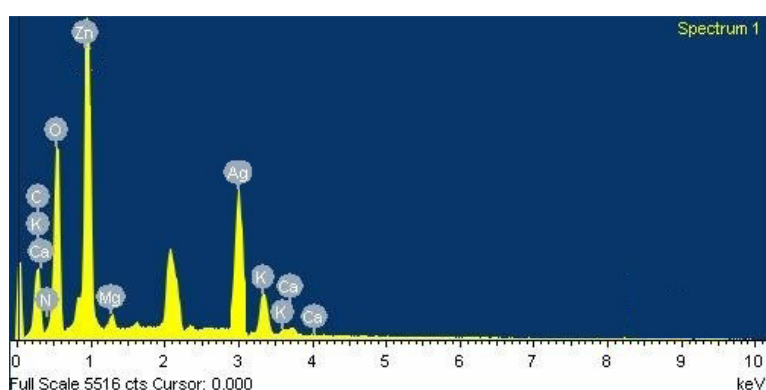


Fig.18 EDS spectrum of Silver nanoparticle

4.6.6 High resolution transmission electron microscopy (HR-TEM) analysis

The HR-TEM images and SAED pattern (**Fig 19**) clearly indicate the shape and size distribution of silver nanoparticle. The images show that the nanoparticles are capped with phytoconstituents. It was observed that the silver nanoparticle formed with random shapes includes spherical, hexagonal, triangular, rod etc. The average size of spherically shaped nanoparticle was found to be 31.31 nm.

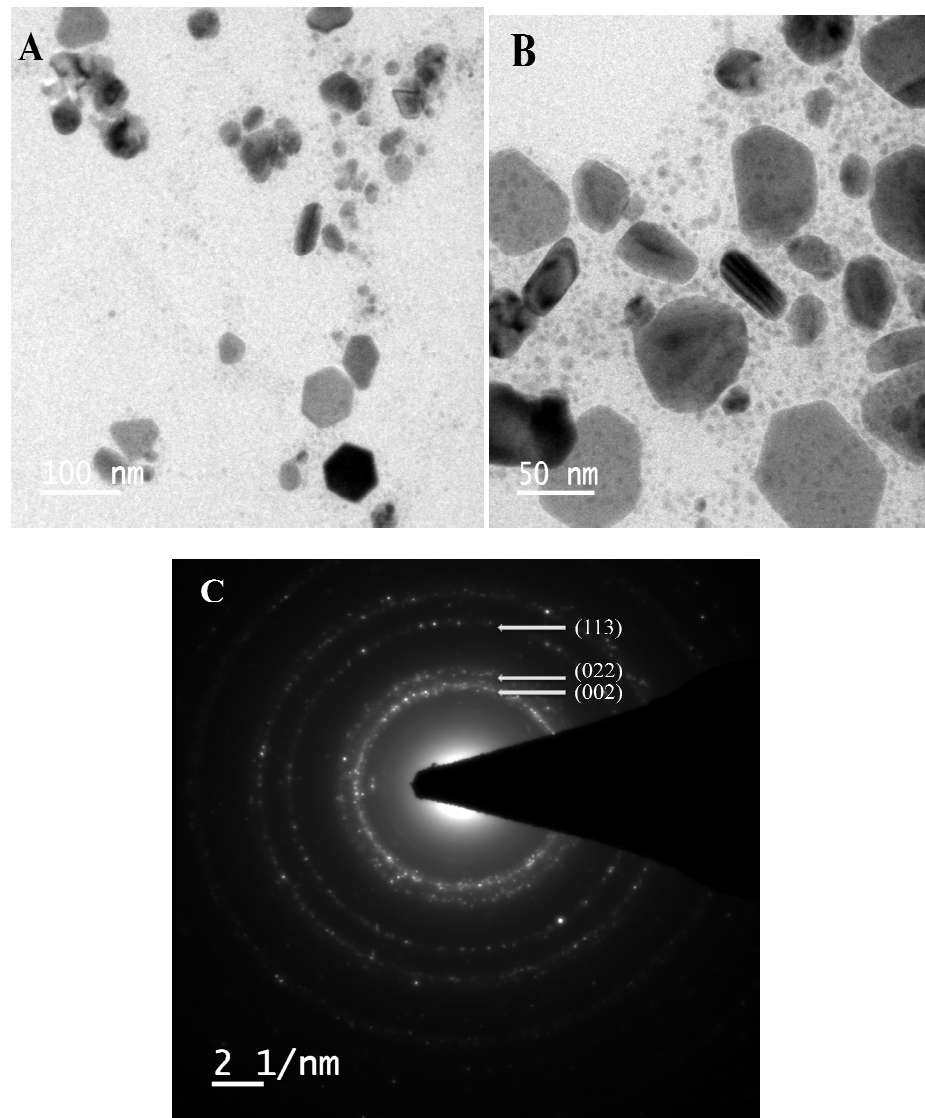


Fig 19 HR-TEM images of silver nanoparticle at different magnification(A&B), SAED pattern(C)

The SAED pattern had ring with bright spots that indicates the nanocrystalline nature of silver nanoparticle. Each ring corresponds to 'd' value and the SAED patterns of (002), (022) and (113) was observed and thus confirms the formation of silver nanoparticle by this method.

4.6.7 Catalytic activity of silver nanoparticle in Azide-Alkyne cycloaddition

The catalytic activity of silver nanoparticle in azide-alkyne cycloaddition reaction was also studied. In a typical reaction, 10 mmol each of benzyl chloride, sodium azide and phenyl acetylene were mixed with 2 mg of the silver nanoparticle as catalyst and heated at 70 °C for 5 h in water. The reaction was monitored by GCMS which shows a slight excess of 1,4-disubstituted-1,2,3-triazole in the product. Retention time of the copper catalysed reaction product 1-benzyl-4-phenyl-1,2,3-triazole (reported in third chapter of this thesis) was used here to differentiate the regioisomers. Optimization of the reaction with respect to solvent system was carried out by using solvents like water, acetic acid, THF, t-BuOH, DMSO, DMF and their binary mixtures (**Scheme 3**). Better yield of the 1,4-regioisomer was obtained when DMSO was used as the solvent (**Entry 6, Table 4**). Our efforts to synthesize either 1,4 or 1,5 regio isomer of the 1,2,3-triazole were not successful.

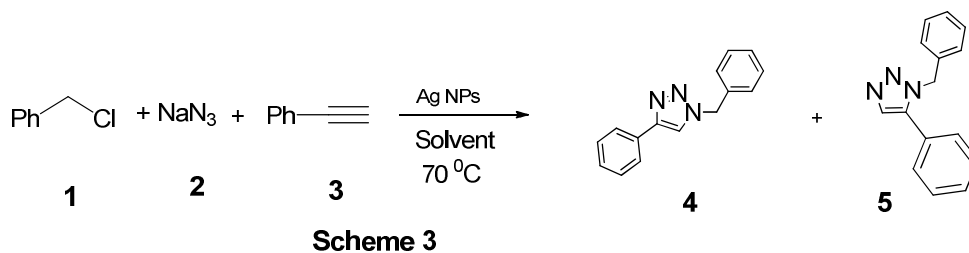


Table 4 Optimization of solvent system for AgAAC reaction

Entry	Solvent	Conversion (4:5)
1	H ₂ O	55:45
2	HAc	60:40
3	t-BuOH/H ₂ O	60:40
4	H ₂ O:THF	55:45
5	THF	65:35
6	DMSO	80:20
7	DMF	70:30

4.6.8 Antibacterial and Antifungal effect of Silver nanoparticle

The antimicrobial activity of silver nanoparticle was tested using well diffusion method against multidrug resistant human pathogens such as gram negative bacteria *Escherichia coli*, *Pseudomonas aeruginosa* and gram positive bacteria *Staphylococcus aureus* and *Bacillus subtilis*(Fig.20). The bacterial culture spread uniformly over the nutrient agar plate and small discs of 3 mm diameter were cut from the surface. To each disc drugs were induced followed by the incubation at 37 °C for 24 h. Then zone of inhibition (mm) was then calculated. The generalized mechanism of interaction of silver ions with phosphorous moieties in DNA leads to the deactivation of DNA replication.^{101,102} Zone of inhibition of silver nanoparticle is given in **Table 5**

Table 5 Zone of inhibition of silver nanoparticle against bacterial strains

Drug (µl)	Zone of Inhibition(mm)			
	<i>Staphylococcus</i> (1)	<i>Bacillus</i> (2)	<i>Pseudomonas</i> (3)	<i>E.coli</i> (4)
Dist. Water	0	0	0	0
Streptomycin	16	22	14	11
50	13	0	13	14
100	15	0	15	15
150	22	10	16	19
200	24	14	21	22

Silver nanoparticle synthesized by green method was found to have better antibacterial activity against *Staphylococcus* (MTCC 3103) with maximum zone of inhibition of 24 mm for 200 µl whereas its effect was low for *Bacillus subtilis*(MTCC 869). 200 µl produces only 14 mm zone of inhibition. For gram negative bacteria *Escherichia coli* (MTCC 68), *Pseudomonas* (MTCC 2642) silver nanoparticle had almost equal activity in all concentrations. Pericarp extract doesn't shows any antibacterial activity against gram positive bacteria *Staphylococcus* and gram negative bacteria *Escherichia coli*.¹⁰³

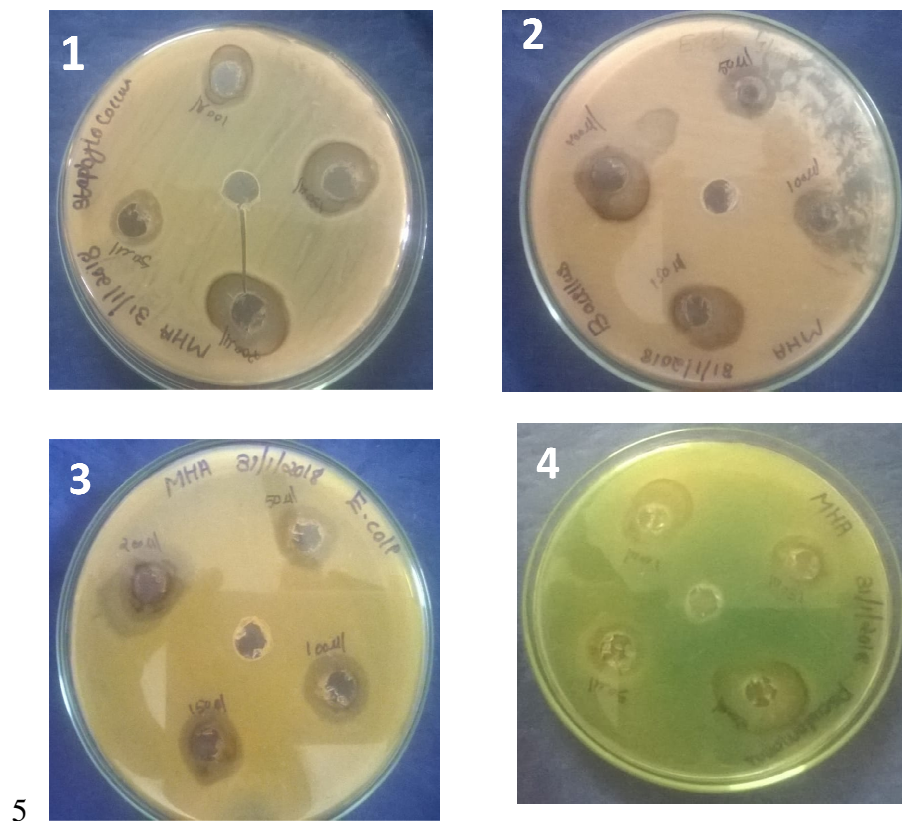


Fig 20 Antimicrobial activity of AgNPs- *Myrsitca fragrans* against human pathogenic microorganisms using agar well diffusion method 1) *Staphylococcus sp.* 2) *Bacillus* 3) *E. coli* 4) *Pseudomonas*

Both surface Plasmon resonance and the antibacterial activity of silver nanoparticle depend on the size of the nanoparticle. When the size of the particle increases the surface plasmon resonance shifted to longer wavelength and the size of nanoparticle signifies that it had large surface area to interact with the microbes.^{104,105} Thus smaller the particle size better will be the interaction. Similarly nanoparticles with different shape do have an effect on antimicrobial activity. Pal reported that for truncated triangular nanoparticle 1 μg quantity show inhibition whereas spherical shaped particle needs a total silver content of 12.5 μg and rod shaped particle needs 50 to 100 μg of silver content.¹⁰⁶

Antifungal activity of silver nanoparticle was measured using the well diffusion method against *Pencillium*, *Aspergillus*, *Rhizopus* and *Curvularia Sp.* Silver nanoparticle shows its activity only against *Pencillium Sp* with a maximum 24 mm of zone of inhibition.

4.7 Experimental details

4.7.1 Preparation of *Myristica fragrans* fruit extract

Around 500 g of fresh matured nutmeg fruit is collected from Nandipulam, Thrissur, Kerala. The fruit is separated from seed and washed with ordinary water. Then it is washed with deionised water 3 times. Then the fruit cut into small pieces and dried well in sun shade for four days, to remove the moisture completely. Dried nutmeg fruit is grounded to powder using a mortar and pestle.

Powdered Nutmeg (10 g) was mixed with distilled water (50 ml) and autoclaved at 110 °C for

2 h. Then allowed to cool to room temperature and filtered through Whatman no.1 filter paper which was then stored at 4 °C.

4.7.2 Green synthesis of CuO nanoparticles

15 mM solution of copper acetate was prepared and stirred at room temperature for 5min followed by the drop wise addition of *Myristica fragrans* fruit extract (about 75 ml). The sample was divided into three portions, one kept for room temperature stirring, another for sonochemical synthesis and the last portion heated in microwave oven for 3 min. the sample under microwave heating produces a sudden color change from blue to green and then a greenish brown colored suspension further heating for 2 min provides black colored residue. The sample kept at room temperature doesn't produce any color change even after 24 h whereas sonicated sample produce a color change after 2 h but further sonication doesn't produce any brown colored suspension. The CuO nanoparticle obtained by microwave heating was recovered by centrifugation and washed with deionized water in order to remove plant biomass. The residue was dried in a vacuum oven at 70 °C for 6 h.

4.7.3 General procedure for azide-alkyne cycloaddition

To a mixture of azide (1.5 mmol), alkyne (1.5 mmol) halides (1 mmol), CuONPs (0.1 g) and distilled water (1 ml) was added. The reaction was conducted both at room temperature for 24 h and by heating at 60 °C for 1 h. Ethyl acetate (1 ml) was added and the organic layer was separated out using extraction. The solvent was evaporated and purified by recrystallization from ethanol. The catalyst was recovered from aqueous layer and dried in vacuum oven at 70 °C for 3 h.

4.7.4 Sunlight mediated synthesis of silver nanoparticle

In a typical procedure, an aqueous solution of silver nitrate (50 ml, 1 mM) was mixed with *Myristica fragrans* (15 ml). The color of the solution remains unchanged when it is kept in dark for 24 h. On exposure to sunlight, the color of the solution changes to yellow and then to reddish brown within 10 min.

4.7.5 Antibacterial activity by well diffusion method

The bacterial cultures were maintained in nutrient broth. Each culture was uniformly distributed on nutrient agar plates. Wells of 3 mm diameter were cut on the surface of nutrient agar plates at a distance of 2 cm using sterile borer. Drugs of different concentrations were added in each well with a micropipette. Then these plates were incubated at 37 °C for 24 h.

4.7.6 Antifungal activity by well diffusion method

The fungal cultures were maintained in SD broth. Each culture was uniformly distributed on nutrient agar plates. Wells of 3mm diameter were cut on the surface of nutrient agar plates at a distance of 2 cm using sterile borer. Drugs of different concentrations were added in each well with a micropipette. These plates were incubated at room temperature for 6-7 days. The incubation of zone diameter was then measured.

4.8 Conclusion

In this chapter, we report eco-friendly and cost effective synthesis of copper oxide and silver nanoparticle using *Myristica fragrans* fruit extract. The CuO nanoparticle showed excellent catalytic activity towards CuAAC reaction and the products obtained in good yield. We have also synthesized silver nanoparticles using the same fruit extract. Silver nanoparticle exhibits better activity against *Staphylococcus*, *Pseudomonas* and *E.Coli* compared to standard Streptomycin

Advantages of using *Myristica fragrans* fruit extract for the synthesis of nanoparticle

- i) Act as stabilizing and reducing agent
- ii) Avoid the use of organic solvents
- iii) Less reaction time

References

- (1) Choi, O.; Kanjun, K.; Kim, N.; Ross, L.; Surampalli, R. Y.; Hu, Z. The Inhibitory Effects of Silver Nanoparticles, Silver Ions, and Silver Chloride Colloids on Microbial Growth. *Water Res.* **2008**, *42*, 3066–3074.
- (2) Jeong, S. H.; Yeo, S. Y.; Yi, S. C. The Effect of Filler Particle Size on the Antibacterial Properties of Compounded Polymer / Silver Fibers. *J. Mater. Sci.* **2005**, *40*, 5407–5411.
- (3) Gawande, M. B.; Goswami, A.; Felpin, F.-X.; Asefa, T.; Huang, X.; Silva, R.; Zou, X.; Zboril, R.; Varma, R. S. Cu and Cu-Based Nanoparticles: Synthesis and Applications in Catalysis. *Chem. Rev.* **2016**, *116*, 3722–3811.
- (4) Das, D. Multicomponent Reactions in Organic Synthesis Using Copper Based Nanocatalyst. *Chem. Sel.* **2016**, *1*, 1959–1980.
- (5) Ranu, B. C.; Dey, R.; Chatterjee, T.; Ahammed, S. Copper Nanoparticle-Catalyzed Carbon–Carbon and Carbon–Heteroatom Bond Formation with a Greener Perspective. *Chem. Sustain. ChemSusChem Energy Mater.* **2012**, *22*–44.
- (6) Indira, K.; Mudali, U. K.; Rajendran, T. N. N. A Review on TiO₂ Nanotubes: Influence of Anodization Parameters, Formation Mechanism, Properties, Corrosion Behavior, and Biomedical Applications. *J. Bio-Tribo-Corrosion* **2015**, *1* (4), 1–22.
- (7) Fathima, J. B.; Pugazhendhi, A.; Venis, R. Synthesis and Characterization of ZrO₂ Nanoparticles-Antimicrobial Activity and Their Prospective Role in Dental Care. *Microb. Pathog.* **2017**, *110*, 245–251.
- (8) Sisubalan, N.; Ramkumar, V. S.; Pugazhendhi, A. ROS-Mediated Cytotoxic Activity of ZnO and CeO₂ Nanoparticles Synthesized Using the Rubia Cordifolia L. Leaf Extract on MG-63 Human Osteosarcoma Cell Lines. *environmental Sci. Pollut. Res.* **2017**, *25*, 10482–10492.
- (9) Liz-marz, L. M. Nanometals: Formation and Color. *Mater. Today* **2004**, 26–

- 31.
- (10) LaMer, V. K.; Dinegar, R. H. Theory, Production and Mechanism of Formation of Monodispersed Hydrosols. *J. Am. Chem. Soc.* **1950**, *72*, 4847–4854.
- (11) Al-thabaiti, S. A.; Obaid, A. Y.; Khan, Z. Formation and Characterization of Surfactant Stabilized Silver Nanoparticles : A Kinetic Study. *Colloids Surfaces B Biointerfaces* **2008**, *67*, 230–237.
- (12) Bajpai, S. K.; Bajpai, M.; Gautam, D. In Situ Formation of Silver Nanoparticles in Hydrogels for Antibacterial Application In Situ Formation of Silver Nanoparticles in Regenerated Cellulose-Polyacrylic Acid (RC-PAAc) Hydrogels for Antibacterial Application. *Pure J. Macromol. Sci. Part A Pure Appl. Chem.* **2013**, *50*, 46–54.
- (13) Esumi, K.; Isono, R.; Yoshimura, T. Preparation of PAMAM - and PPI - Metal (Silver , Platinum , and Palladium) Nanocomposites and Their Catalytic Activities for Reduction of 4-Nitrophenol. *Langmuir* **2004**, *20*, 237–243.
- (14) Yin, B.; Ma, H.; Wang, S.; Chen, S. Electrochemical Synthesis of Silver Nanoparticles under Protection of Poly (N -Vinylpyrrolidone). *J. Phys. Chem. B* **2003**, *107*, 8898–8904.
- (15) Mayya, K. S.; Schoeler, B.; Caruso, F. Preparation and Organization of Nanoscale Polyelectrolyte-Coated Gold Nanoparticle. *Adv. Funct. Mater.* **2003**, *13*, 183–188.
- (16) Liu, M.; Lin, M. C.; Tsai, C. Y.; Wang, C. Enhancement of Thermal Conductivity with Cu for Nanofluids Using Chemical Reduction Method. *Int. J. Heat Mass Transf.* **2006**, *49*, 3028–3033.
- (17) Khanna, P. K.; Gaikwad, S.; Adhyapak, P. V; Singh, N.; Marimuthu, R. Synthesis and Characterization of Copper Nanoparticles. *Mater. Lett.* **2007**, *61*, 4711–4714.
- (18) Pillai, Z. S.; Kamat, P. V. What Factors Control the Size and Shape of Silver Nanoparticles in the Citrate Ion Reduction Method ? *J. Phys. Chem. B* **2004**, *108*, 945–951.

- (19) Dong, X.; Ji, X.; Wu, H.; Zhao, L.; Li, J.; Yang, W. Shape Control of Silver Nanoparticles by Stepwise Citrate Reduction. *J. Phys. Chem. C* **2009**, *113*, 6573–6576.
- (20) Ledwith, D. M.; Whelan, A. M.; Kelly, J. M. A Rapid , Straight-Forward Method for Controlling the Morphology of Stable Silver Nanoparticles. *J. Mater. Chem.* **2007**, *17*, 2459–2464.
- (21) Turkevich, J.; Stevenson, P. C.; Hillier, J. A Study of the Nucleation and Growth Processes in the Synthesis of Colloidal Gold. *Discuss. Faraday Soc.* **1951**, *11*, 55–75.
- (22) Xia, H.; Bai, S.; Hartmann, J.; Wang, D. Synthesis of Monodisperse Quasi-Spherical Gold Nanoparticles in Water via Silver (I) -Assisted Citrate Reduction. *Langmuir* **2010**, *26*, 3585–3589.
- (23) Stevenson, A. P. Z.; Bea, D. B.; Civit, S.; Contera, S. A.; Cerveto, A. I.; Trigueros, S. Three Strategies to Stabilise Nearly Monodispersed Silver Nanoparticles in Aqueous Solution. *Nanoscale Res. Lett.* **2012**, *7*, 1–8.
- (24) Krutyakov, Y. A.; Kudrinskiy, A. A.; Olenin, A. Y.; Lisichkin, G. V. Synthesis and Properties of Silver Nanoparticles : Advances and Prospects. *Russ. Chem. Rev.* **2008**, *77*, 233–257.
- (25) Qing-ming, L. I. U.; De-bi, Z.; Yamamoto, Y.; Ichino, R.; Okido, M. Preparation of Cu Nanoparticles with NaBH₄ by Aqueous Reduction Method. *Trans. Nonferrous Met. Soc. China* **2012**, *22*, 117–123.
- (26) Samal, A. K.; Sreepasad, Æ. T. S. Investigation of the Role of NaBH₄ in the Chemical Synthesis of Gold Nanorods. *J. Nanoparticle Res.* **2010**, *12*, 1777–1786.
- (27) Sun, Y.; Xia, Y. Large-Scale Synthesis of Uniform Silver Nanowires Through a Soft, Self-Seeding, Polyol Process. *Adv. Mater.* **2002**, *14*, 833–837.
- (28) Kawasaki, H. Surfactant-Free Solution-Based Synthesis of Metallic Nanoparticles toward Efficient Use of the Nanoparticles ' Surfaces and Their Application in Catalysis and Chemo- / Biosensing. *Nanotechnol. Rev.* **2013**, *2*,

5–25.

- (29) Kim, D.; Jeong, S.; Moon, J. Synthesis of Silver Nanoparticles Using the Polyol Process and the Influence of Precursor Injection. *Nanotechnology* **2006**, *17*, 4019–4024.
- (30) Zain, N. M.; Stapley, A. G. F.; Shama, G. Green Synthesis of Silver and Copper Nanoparticles Using Ascorbic Acid and Chitosan for Antimicrobial Applications. *Carbohydr. Polym.* **2014**, 195–202.
- (31) Biçer, M.; İlkay Şişman. Controlled Synthesis of Copper Nano / Microstructures Using Ascorbic Acid in Aqueous CTAB Solution. *Powder Technol.* **2010**, *198*, 279–284.
- (32) Qing-ming, L. I. U.; Yasunami, T.; Kuruda, K.; Okido, M. Preparation of Cu Nanoparticles with Ascorbic Acid by Aqueous Solution Reduction Method. *Trans. Nonferrous Met. Soc. China* **2012**, *22* (9), 2198–2203.
- (33) Xiong, J.; Wang, Y.; Xue, Q.; Wu, X. Synthesis of Highly Stable Dispersions of Nanosized Copper Particles Using L -Ascorbic Acid. *Green Chem.* **2011**, *13*, 900–904.
- (34) Lee, Y.; Choi, J.; Lee, K. J.; Stott, N. E.; Kim, D. Large-Scale Synthesis of Copper Nanoparticles by Chemically Controlled Reduction for Applications of Inkjet-Printed Electronics. *Nanotechnology* **2008**, *415604*, 1–7.
- (35) Dang, T. M. D.; Le, T. T. T.; Fribourg-Blanc, E.; Dang, M. C. The Influence of Solvents and Surfactants on the Preparation of Copper Nanoparticles by a Chemical Reduction Method. *Adv. Nat. Sci. Nanosci. Nanotechnol.* **2011**, *2*.
- (36) Pastoriza-santos, B. I.; Liz-marza, L. M. N , N -Dimethylformamide as a Reaction Medium for Metal Nanoparticle Synthesis. *Adv. Funct. Mater.* **2009**, *19*, 679–688.
- (37) Pastoriza-santos, I.; Liz-marzán, L. M. Reduction of Silver Nanoparticles in DMF . Formation of Monolayers and Stable Colloids. *Pure Appl. Chem.* **2000**, *72*, 83–90.

- (38) Gonz, R.; Del, G.; Rodr, M.; Primera-pedrozo, O. M.; Carlos, R.; Hern, S. P. Improving SERS Detection of *Bacillus Thuringiensis* Using Silver Nanoparticles Reduced with Hydroxylamine and with Citrate Capped Borohydride. *Int. J. Spectroscopy* **2011**, *2011*, 1–9.
- (39) Zhang, W.; Qiao, X.; Chen, J. Synthesis of Silver Nanoparticles — Effects of Concerned Parameters in Water/Oil Microemulsion. *Mater. Sci. Eng. B* **2007**, *142*, 1–15.
- (40) Gutierrez, M.; Henglein, A.; Dohrmann, J. K. Hydrogen Atom Reactions in the Sonolysis of Aqueous Solutions. *J. Phys. Chem.* **1987**, *91*, 6687–6690.
- (41) Dhas, N. A.; Raj, C. P.; Gedanken, A. Synthesis , Characterization , and Properties of Metallic Copper Nanoparticles. *Chem. Mater.* **1998**, *10*, 1446–1452.
- (42) Kumar, R. V.; Mastai, Y.; Diamant, Y.; Gedanken, A. Sonochemical Synthesis of Amorphous Cu and Nanocrystalline Cu₂O Embedded in Polianiline Matrix. *J. Mater. Chem.* **2001**, *11*, 1209–1213.
- (43) Salkar, R. A.; Jeevanandam, P.; Aruna, S. T.; Koltypin, Y.; Gedanken, A. The Sonochemical Preparation of Amorphous Silver Nanoparticles. *J. Mater. Chem.* **1999**, *9*, 1333–1335.
- (44) Giuffrida, S.; Costanzo, L. L.; Ventimiglia, G.; Bongiorno, C. Photochemical Synthesis of Copper Nanoparticles Incorporated in Poly (Vinyl Pyrrolidone). *J. Nanoparticle Res.* **2008**, *10*, 1183–1192.
- (45) Klaus, T.; Joerger, R.; Olsson, E.; Granqvist, C.-G. Silver-Based Crystalline Nanoparticles, Microbially Fabricated. *Proc. Natl. Acad. Sci. United States Am.* **1999**, *96*, 13611–13614.
- (46) Shahverdi, A. R.; Minaeian, S.; Reza, H.; Jamalifar, H.; Nohi, A. Rapid Synthesis of Silver Nanoparticles Using Culture Supernatants of Enterobacteria: A Novel Biological Approach. *Process Biochem.* **2007**, *42*, 919–923.
- (47) Fayaz, A. M.; Girilal, M.; Rahman, M.; Venkatesan, R.; Kalaichelvan, P. T.

- Biosynthesis of Silver and Gold Nanoparticles Using Thermophilic Bacterium *Geobacillus Stearothermophilus*. *Process Biochem.* **2011**, *46*, 1958–1962.
- (48) Kalishwaralal, K.; Deepak, V.; Ram, S.; Pandian, K.; Kottaisamy, M.; Barathmanikant, S.; Kartikeyan, B.; Gurunathan, S. Biosynthesis of Silver and Gold Nanoparticles Using *Brevibacterium Casei*. *Colloids Surfaces B Biointerfaces* **2010**, *77*, 257–262.
- (49) Lakshmi, V.; Roshmi, D.; Varghese, R. T.; Soniya, E. V.; Mathew, J.; Radhakrishnan, E. K. Extracellular Synthesis of Silver Nanoparticles by the *Bacillus* Strain CS 11 Isolated from Industrialized Area. *3Biotech* **2014**, *4*, 121–126.
- (50) Mukherjee, P.; Ahmad, A.; Mandal, D.; Senapati, S.; Sainkar, S. R.; Khan, M. I.; Parishcha, R.; Ajaykumar, P. V.; Alam, M.; Kumar, R.; et al. Fungus-Mediated Synthesis of Silver Nanoparticles and Their Immobilization in the Mycelial Matrix : A Novel Biological Approach to Nanoparticle Synthesis. *Nano Lett.* **2001**, *1*, 515–519.
- (51) Ahmad, A.; Mukherjee, P.; Senapati, S.; Mandal, D.; Khan, M. I.; Sastry, M. Extracellular Biosynthesis of Silver Nanoparticles Using the Fungus *Fusarium Oxysporum*. *Colloids Surfaces B Biointerfaces* **2003**, *28*, 313–318.
- (52) Kumar, S. A.; Abyaneh, M. K.; Gosavi, S. W.; Kulkarni, S. K.; Pasricha, R.; Ahmad, A.; Khan, M. I. Nitrate Reductase-Mediated Synthesis of Silver Nanoparticles from $AgNO_3$. *Biotechnol. Lett.* **2007**, *29*, 439–445.
- (53) Kathiresan, K.; Manivannan, S.; Nabeel, M. A.; Dhivya, B. Studies on Silver Nanoparticles Synthesized by a Marine Fungus , *Penicillium Fellutanum* Isolated from Coastal Mangrove Sediment. *Colloids Surfaces B Biointerfaces* **2009**, *71*, 133–137.
- (54) Kasthuri, J.; Kathiravan, K.; Rajendran, N. Phyllanthin-Assisted Biosynthesis of Silver and Gold Nanoparticles : A Novel Biological Approach. *J. Nanoparticle Res.* **2009**, *11*, 1075–1085.
- (55) Iram, F.; Iqbal, M. S.; Athar, M. M.; Saeed, M. Z.; Yasmeen, A.; Ahmad, R.

- Glucosylan-Mediated Green Synthesis of Gold and Silver Nanoparticles and Their Phyto-Toxicity Study. *Carbohydr. Polym.* **2014**, *104*, 29–33.
- (56) Durai, P.; Arulvasu, C.; Gajendran, B.; Ramar, M. Synthesis and Characterization of Silver Nanoparticles Using Crystal Compound of Sodium Para-Hydroxybenzoate Tetrahydrate Isolated from Vitex Negundo . L Leaves and Its Apoptotic Effect on Human Colon Cancer Cell Lines. *Eur. J. Med. Chem.* **2014**, *84*, 90–99.
- (57) Kasthuri, J.; Veerapandian, S.; Rajendiran, N. Biological Synthesis of Silver and Gold Nanoparticles Using Apiin as Reducing Agent. *Colloids Surfaces B Biointerfaces* **2009**, *68*, 55–60.
- (58) Ahmed, K. B. A.; Subramaniam, S.; Veerappan, G.; Hari, N.; Aravind Sivasubramanian, A. V. β -Sitosterol-D-Glucopyranoside Isolated from Desmostachya Bipinnata Mediate Photoinduced Rapid Green Synthesis of Silver Nanoparticles. *RSC Adv.* **2014**, *4*, 59130–59136.
- (59) Basha, S. K.; Govindaraju, K.; Manikandan, R.; Ahn, J. S.; Bae, E. Y.; Singaravelu, G. Phytochemical Mediated Gold Nanoparticles and Their PTP 1B Inhibitory Activity. *Colloids Surfaces B Biointerfaces* **2010**, *75*, 405–409.
- (60) Gardea-torresdey, J. L.; Gomez, E.; Peralta-videa, J. R.; Parsons, J. G.; Troiani, H.; Jose-yacaman, M. Alfalfa Sprouts : A Natural Source for the Synthesis of Silver Nanoparticles. *Langmuir* **2003**, *19*, 1357–1361.
- (61) Harris, A. T.; Bali, R. On the Formation and Extent of Uptake of Silver Nanoparticles by Live Plants. *J. Nanoparticle Res.* **2008**, *10*, 691–695.
- (62) Sharma, N. C.; Torresdey, J. L. G.-. Synthesis of Plant-Mediated Gold Nanoparticles and Catalytic Role of Biomatrix-Embedded Nanomaterials. *Environ. Sci. Technol.* **2007**, *41*, 5137–5142.
- (63) Rodriguez, J. L. G. Æ. E.; Peralta-videa, J. G. P. Æ. J. R.; Cruz-jimenez, G. M. Æ. G. Use of ICP and XAS to Determine the Enhancement of Gold Phytoextraction by Chilopsis Linearis Using Thiocyanate as a Complexing Agent. *Anal. Bioanal. Chem.* **2005**, *382*, 347–352.

- (64) Ibrahim, H. M. M. Synthesis and Characterization of Silver Nanoparticles Using Banana Peel Extract and Their Antimicrobial Activity against Representative Microorganisms. *J. Radiat. Res. Appl. Sci.* **2015**, *8*, 265–275.
- (65) Sharma, G.; Sharma, A. R.; Kurian, M.; Bhavesh, R.; Nam, J. S.; Lee, S. S. Green Synthesis of Silver Nanoparticle Using Myristica Fragrans(Nutmeg) Seed Extract and Its Biological Activity. *Dig. J. Nanomater. Biostructures* **2014**, *9*, 325–332.
- (66) Elavazhagan, T.; Arunachalam, K. D. Memecylon Edule Leaf Extract Mediated Green Synthesis of Silver and Gold Nanoparticles. *Int. J. Nanomedicine* **2011**, *6*, 1265–1278.
- (67) Singh, A.; Jain, D.; Upadhyay, M. K.; Khandelwal, N. Green Synthesis of Silver Nanoparticles Using Argemone Mexicana Leaf Extract and Evaluation of Their Antimicrobial Activities. *Dig. J. Nanomater. Biostructures* **2010**, *5*, 483–489.
- (68) Jain, D.; Daima, H. K.; Kachhwaha, S.; Kothari, S. L. Synthesis of Plant Mediated Silver Nanoparticles Using Papaya Fruit Extract and Evaluation of Their Antimicrobial Activities. *Dig. J. Nanomater. Biostructures* **2009**, *4*, 557–563.
- (69) Savithramma, P. Y. N. Biosynthesis , Characterization and Antimicrobial Studies of Green Synthesized Silver Nanoparticles from Fruit Extract of Syzygium Alternifolium (Wt .) Walp . an Endemic , Endangered Medicinal Tree Taxon. *Appl. Nanosci.* **2016**, *6*, 223–233.
- (70) Rao, Y. S.; Kotakadi, V. S.; Prasad, T. N. V. K. V; Reddy, A. V; Gopal, D. V. R. S. Green Synthesis and Spectral Characterization of Silver Nanoparticles from Lakshmi Tulasi (Ocimum Sanctum) Leaf Extract. *Spectrochem. Acta PartA Mol. Biomolecular Spectrosc.* **2013**, *103*, 156–159.
- (71) Ahmed, S.; Saifullah; Ahmad, M.; Swami, B. L. Green Synthesis of Silver Nanoparticles Using Azadirachta Indica Aqueous Leaf Extract. *J. Radiat. Res. Appl. Sci.* **2015**, *9*, 1–7.

- (72) Velu, K.; Elumalai, D.; Hemalatha, P.; Janaki, A. Evaluation of Silver Nanoparticles Toxicity of Arachis Hypogaea Peel Extracts and Its Larvicidal Activity against Malaria and Dengue Vectors. *environmental Sci. Pollut. Res.* **2015**, *22*, 17769–17779.
- (73) Zaheer, Z. Biogenic Synthesis, Optical, Catalytic, and in Vitro Antimicrobial Potential of Ag Nanoparticles Prepared Using Palm Date Fruit Extract. *J. Photochem. Photobiol. B Biol.* **2018**, *178*, 584–592.
- (74) Nisha, S. N.; Aysha, O. S.; Nasar, J. S.; Kumar, P. V.; Valli, S.; Nirmala, P.; Reena, A. Lemon Peels Mediated Synthesis of Silver Nanoparticles and Its Antidermatophytic Activity. *Spectrochim. Acta Part A Mol. Biomol. Spectrosc.* **2014**, *124*, 194–198.
- (75) Ahamed, M.; M.A.MajeedKhan; M.K.J.Siddiqui; S.AISalhi, M.; SalmanA.Alrokayan. Green Synthesis , Characterization and Evaluation of Biocompatibility of Silver Nanoparticles. *Phys. E Low-dimensional Syst. Nanostructures* **2011**, *43*, 1266–1271.
- (76) Shende, S.; Ingle, A. P.; Gade, A.; Rai, M. Green Synthesis of Copper Nanoparticles by Citrus Medica Linn.(Idilimbu) Juice and Its Antimicrobial Activity. *World J. Microbiol. Biotechnol.* **2015**, *31*, 865–873.
- (77) Harne, S.; Sharma, A.; Dhaygude, M.; Joglekar, S.; Kodam, K. Novel Route for Rapid Biosynthesis of Copper Nanoparticles Using Aqueous Extract of Calotropis Procera L . Latex and Their Cytotoxicity on Tumor Cells. *Colloids Surfaces B Biointerfaces* **2012**, *95*, 284–288.
- (78) Lee, H.; Song, J. Y.; Kim, B. S. Biological Synthesis of Copper Nanoparticles Using Magnolia Kobus Leaf Extract and Their Antibacterial Activity. *Chem. Technol. Biotechnol.* **2013**, *88*, 1971–1977.
- (79) Nasrollahzadeh, M.; Sajadi, S. M. Green Synthesis of Copper Nanoparticles Using Ginkgo Biloba L . Leaf Extract and Their Catalytic Activity for the Huisgen [3 + 2] Cycloaddition of Azides and Alkynes at Room Temperature. *J. Colloid Interface Sci.* **2015**, *457*, 141–147.

- (80) Nasrollahzadeh, M.; Sajadi, S. M.; Mehdi Khalaj. Green Synthesis of Copper Nanoparticles Using Aqueous Extract of the Leaves of Euphorbia Esula L and Their Catalytic Activity for Ligand-Free Ullmann-Coupling Reaction and Reduction of 4-Nitrophenol. *RSC Adv.* **2014**, *4*, 47313–47318.
- (81) Mukhopadhyay, R.; Kazi, J.; Debnath, M. C. Synthesis and Characterization of Copper Nanoparticles Stabilized with Quisqualis Indica Extract : Evaluation of Its Cytotoxicity and Apoptosis in B16F10 Melanoma Cells. *Biomed. Pharmacother.* **2018**, *97*, 1373–1385.
- (82) Nazar, N.; Bibi, I.; Kamal, S.; Iqbal, M.; Nouren, S.; Jalani, K.; Umair, M.; Atta, S. Cu Nanoparticles Synthesis Using Biological Molecule of P. Granatum Seeds Extract as Reducing and Capping Agent: Growth Mechanism and Photo-Catalytic Activity. *Int. J. Biol. Macromol.* **2017**, *106*, 1203–1210.
- (83) Ghidan, A. Y.; Al-antary, T. M.; Awwad, A. M. Green Synthesis of Copper Oxide Nanoparticles Using Punica Granatum Peels Extract : Effect on Green Peach Aphid. *Environ. Nanotechnology, Monit. & Manag.* **2016**, *6*, 95–98.
- (84) Sivaraj, R.; Rahman, P. K. S. M.; Rajiv, P.; Abdul, H.; Venckatesh, R. Biogenic Copper Oxide Nanoparticles Synthesis Using Tabernaemontana Divaricate Leaf Extract and Its Antibacterial Activity against Urinary Tract Pathogen. *Spectrochim. Acta Part A Mol. Biomol. Spectrosc.* **2014**, *133*, 178–181.
- (85) Nasrollahzadeh, M.; Momeni, S. S.; Sajadi, S. M. Green Synthesis of Copper Nanoparticles Using Plantago Asiatica Leaf Extract and Their Application for the Cyanation of Aldehydes Using K₄Fe (CN)₆. *J. Colloid Interface Sci.* **2017**, *506*, 471–477.
- (86) Abdul, M.; Naikodi, R.; Waheed, M. A.; Shareef, M. A.; Ahmad, M.; Nagaiah, K. Standardization of the Unani Drug – Myristica Fragrans Hoult . (Javetri) – with Modern Analytical Techniques. *Pharm. Methods* **2011**, *2*, 76–82.
- (87) Bindu, N. H. S. A. I.; Kumar, S. R. In-Vitro Assimilation of Trimyristin in the Seeds of Myristica Fragrans and in Poly Herbal Ayurvedic Formulation by

- UFLC Method. *Asian J. Pharm. Clin. Res.* **2014**, *6*, 140–145.
- (88) Mittal, A. K.; Chisti, Y.; Banerjee, U. C. Synthesis of Metallic Nanoparticles Using Plant Extracts. *Biotechnol. Adv.* **2013**, *31*, 346–356.
- (89) Thakkar, K. N.; Mhatre, S. S.; Parikh, R. Y. Biological Synthesis of Metallic Nanoparticles. *Nanomedicine Nanotechnology, Biol. Med.* **2010**, *6*, 257–262.
- (90) Nasrollahzadeh, M.; Maham, M.; Sajadi, S. M. Green Synthesis of CuO Nanoparticles by Aqueous Extract of *Gundelia Tournefortii* and Evaluation of Their Catalytic Activity for the Synthesis of N -Monosubstituted Ureas and Reduction of 4-Nitrophenol. *J. Colloid Interface Sci.* **2015**, *455*, 245–253.
- (91) Tamuly, C.; Hazarika, M.; Ch, S.; Das, M. R.; Boruah, M. P. In Situ Biosynthesis of Ag , Au and Bimetallic Nanoparticles Using Piper *Pedicellatum* C . DC : Green Chemistry Approach. *Colloids Surfaces B Biointerfaces* **2013**, *102*, 627–634.
- (92) Pandey, R.; Mahar, R.; Hasanain, M.; Shukla, S. K. Rapid Screening and Quantitative Determination of Bioactive Compounds from Fruit Extracts of *Myristica* Species and Their In-Vitro Antiproliferative Activity. *Food Chem.* **2016**, *211*, 483–493.
- (93) Pandey, R.; Rameshkumar, K. B.; Kumar, B. Ultra High Performance Liquid Chromatography Tandem Mass Spectrometry Method for the Simultaneous Determination of Multiple Bioactive Constituents in Fruit Extracts of *Myristica* Fragrans and Its Marketed Multi-Herbal Formulations Using a Polarity Switchin. *J. Sep. Sci.* **2015**, *38*, 1277–1285.
- (94) Singh, A. K.; Talat, M.; Singh, D. P.; Srivastava, O. N. Biosynthesis of Gold and Silver Nanoparticles by Natural Precursor Clove and Their Functionalization with Amine Group. *J. Nanoparticle Res.* **2010**, *12*, 1667–1675.
- (95) Jiang, X.; Herricks, T.; Xia, Y. CuO Nanowires Can Be Synthesized by Heating Copper Substrates in Air. *Nano Lett.* **2002**, *2*, 1334–1338.
- (96) Creary, X.; Anderson, A.; Brophy, C.; Crowell, F.; Funk, Z. Method for

- Assigning Structure of 1,2,3-Triazoles. *J. Org. Chem.* **2012**, *77*, 8756–8761.
- (97) Ahmed, K. B. A.; Senthilnathan, R.; Megarajan, S.; Anbazhagan, V. Sunlight Mediated Synthesis of Silver Nanoparticles Using Redox Phytoprotein and Their Application in Catalysis and Colorimetric Mercury Sensing. *J. Photochem. Photobiol. B Biol.* **2015**, *151*, 39–45.
- (98) Ulug, B.; Turkdemir, M. H.; Cicek, A.; Mete, A. Role of Irradiation in the Green Synthesis of Silver Nanoparticles Mediated by Fig (*Ficus Carica*) Leaf Extract. *Spectrochem. Acta Part A Mol. Biomol. Spectrosc.* **2015**, *135*, 153–161.
- (99) Manikprabhu, D.; Cheng, J.; Chen, W.; Kumar, A.; Mane, S. B.; Kumar, R.; Hozzein, W. N.; Duan, Y.; Li, W. Sunlight Mediated Synthesis of Silver Nanoparticles by a Novel Actinobacterium (*Sinomonas Mesophila* MPKL 26) and Its Antimicrobial Activity against Multi Drug Resistant *Staphylococcus Aureus*. *J. Photochem. Photobiol. B Biol.* **2016**, *158*, 202–205.
- (100) Magudapathy, P.; Gangopadhyay, P.; Panigrahi, B. K.; Nair, K. G. M.; Dhara, S. Electrical Transport Studies of Ag Nanoclusters Embedded in Glass Matrix. *Phys. B* **2001**, *299*, 142–146.
- (101) Lansdown, A. B. G. Silver I: Its Antibacterial Properties and Mechanism of Action. *J. Wound Care* **1970**, *11*, 125–130.
- (102) Castellano, J. J.; Shafii, S. M.; Ko, F.; Donate, G.; Wright, T. E.; Mannari, R. J.; Payne, W. G.; Smith, D. J.; Jj, C.; Sm, S.; et al. Comparative Evaluation of Silver-Containing Antimicrobial Dressings and Drugs. *Int. Wound J.* **2007**, *4*, 114–122.
- (103) Sulaiman, S. F.; Ooi, K. L. Antioxidant and Anti Food-Borne Bacterial Activities of Extracts from Leaf and Different Fruit Parts of *Myristica Fragrans* Houtt. *Food Control* **2012**, *25*, 533–536.
- (104) Mulvaney, P. Surface Plasmon Spectroscopy of Nanosized Metal Particles. *Langmuir* **1996**, No. 12, 788–800.
- (105) Morones, J. R.; Elechiguerra, J. L.; Camacho, A.; Holt, K.; Kouri, J. B.; Ram, J. T.; Yacaman, M. J. The Bactericidal Effect of Silver Nanoparticles.

Nanotechnology **2005**, *16*, 2346–2353.

- (106) Pal, S.; Tak, Y. K.; Song, J. M. Does the Antibacterial Activity of Silver Nanoparticles Depend on the Shape of the Nanoparticle ? A Study of the Gram-Negative Bacterium *Escherichia Coli* . *Appl. Environmental Microbiol.* **2007**, *73*, 1712–1720.